



STRATIGRAPHY AND PETROLOGY OF THE UWEKAHUNA BLUFF SECTION, KILAUEA CALDERA

By Thomas J. Casadevall and Daniel Dzurisin

ABSTRACT

Samples from 63 lava flows in a 135-m vertical section at Uwekahuna Bluff within Kilauea caldera were analyzed for major oxides, trace elements, and rare-earth elements. Four stratigraphically defined suites of subaerial lava flows are present: (A) units 1–14 (youngest suite), plagioclase-porphyrific flows (6.4–7.3 weight percent MgO); (B) units 15–30, aphyric flows (6.5–8.0 weight percent MgO); (C) units 31–51, olivine-rich flows (9.0–19.7 weight percent MgO) with the Uwekahuna Ash Member of the Puna Basalt at base; (D) units 44A–52A (oldest suite), nonvesicular, aphyric flows (7.1–7.8 weight percent MgO).

Suite D flows were erupted at about 2.8 ka, probably in an ancient caldera. At about 2.1 ka, catastrophic eruption of the Uwekahuna Ash Member may have unloaded Kilauea's deep magma-transport system and triggered extrusion of olivine-porphyrific lavas of suite C. Suites A and B may be genetically related, possibly from the top of a single reservoir; the plagioclase-porphyrific flows of suite A may represent the later eruptive product of a shallow reservoir that earlier was the source for the aphyric lavas of suite B. We interpret this sequence of aphyric lavas followed by plagioclase-porphyrific lavas as indicating a two-stage drawdown of a post-Uwekahuna Ash Member magma reservoir.

Comparison of published major- and trace-element data from Kilauea and Mauna Loa with data for the Uwekahuna Bluff flows indicates the latter are all from a Kilauea source; apparently no Mauna Loa flows occur in the west wall of Kilauea caldera, although surface flows from Mauna Loa have been mapped within 1 km of the caldera rim.

INTRODUCTION

Kilauea Volcano, on the southeast flank of much larger Mauna Loa Volcano (fig. 13.1), has a broad, gently sloping summit region 1,260 m above sea level and two rift zones that extend outward from a 3 × 5-km summit caldera. The western wall of Kilauea caldera is easily accessible and contains the largest cross-sectional exposure of the summit area (fig. 13.1). This exposure comprises numerous lava flows, at least 18 dikes (Casadevall and Dzurisin, chapter 14), the Uwekahuna laccolith (Murata and Richter, 1961), and three pyroclastic units—the A.D. 1924 lithic ash and the mostly A.D. 1790 Keanakakoi and 2.1-ka Uwekahuna Ash Members of the Puna Basalt (Powers, 1948; Dzurisin and Casadevall, 1986; Lockwood and Rubin, 1986). The wall extends from the area

known as the Outlet roughly 6 km northward to the Steaming Bluff area and includes the 135-m-high Uwekahuna Bluff (fig. 13.2). From Uwekahuna Bluff north to Steaming Bluff, the western wall is an unbroken and near-vertical slice through the summit area of Kilauea shield (fig. 13.1). South of Uwekahuna Bluff, however, the wall has a stepped profile attributed to normal faulting (Dutton, 1884; Peterson, 1967; Holcomb, 1981; de Saint Ours, 1982).

We report here the results of field and laboratory studies of rocks in the Uwekahuna Bluff area of Kilauea's summit caldera. Using chemistry, field occurrence, and petrography, we distinguish flows and attempt to identify systematic chemical variations in the composition of summit lava flows. We have examined the data to see whether they allow extension of the secular chemical variation recognized for historical flows (Wright, 1971) further back in time and to see whether they support the hypothesis that more than one long-lived eruptive center was active in the Kilauea summit area during the past several thousand years (Holcomb, 1981).

Considering the proximity of Mauna Loa surface lavas to the present western rim of Kilauea caldera (Peterson, 1967; J.P. Lockwood, written commun., 1980), we have also scrutinized the data to determine if any flow at Uwekahuna Bluff might have come from Mauna Loa. Previous work has suggested that historical lavas from Kilauea and Mauna Loa can be distinguished by major-element chemistry (Powers, 1955; Wright, 1971; Basaltic Volcanism Study Project, 1981) and rare-earth-element chemistry (Leeman and others, 1977, 1980; Basaltic Volcanism Study Project, 1981).

This study is a companion to two others conducted concurrently. One focuses on the age, distribution, and eruptive mechanism of the Uwekahuna Ash Member of the Puna Basalt, a product of large phreatomagmatic eruptions in the Kilauea summit area (Dzurisin and Casadevall, 1986; Lockwood and Rubin, 1986). The other describes the distribution and petrology of intrusive bodies in Kilauea caldera and assesses the importance of intrusions to the growth of the summit region of Kilauea (Casadevall and Dzurisin, chapter 14).

PREVIOUS STUDIES

Although geologic mapping of Kilauea's summit area has focused on young surface flows (Peterson, 1967; Walker, 1969;



FIGURE 13.1.—Aerial view looking southwest over Kilauea caldera toward the east flank of Mauna Loa, showing location of Uwekahuna Bluff section and Hawaiian Volcano Observatory (HVO). Photograph by J.P. Lockwood, U.S. Geological Survey.

Holcomb, 1981) and on the structural setting of the summit region (de Saint Ours, 1982), some studies have concerned the walls of the caldera and nearby pit craters. Macdonald described the sequence of flows exposed at Uwekahuna Bluff (Stearns and Macdonald, 1946; Macdonald, 1949), Doell sampled the Uwekahuna section for paleomagnetic studies (Doell and Cox, 1965, 1972), and Wright (1971) reported on the chemistry of several of Doell's samples.

Stearns and Macdonald (1946, p. 99–111) placed the three widespread tephra deposits at Kilauea into a stratigraphic framework for the volcano. The Uwekahuna Ash Member of the Puna Basalt is the oldest at 2.1 ka (Lockwood and Rubin, 1986). At Uwekahuna Bluff the ash is overlain by 105–135 m of lava flows, capped by the mostly A.D. 1790 Keanakakoi Ash Member and by traces of A.D. 1924 lithic ash.

ACKNOWLEDGMENTS

We greatly appreciate the interest and advice received from many colleagues, in particular T.L. Wright, which have been helpful in clarifying our ideas. We also wish to thank J. Arth, D.E. Champion, D.A. Clague, R.T. Holcomb, J.P. Lockwood, D.W. Peterson, D.A. Swanson, and R.I. Tilling. Initial thin section descriptions and point counts for figure 13.4 were made by J.E. Ewert. Major-element chemistry was determined by J. Reid and D. Kay; instrumental neutron activation analyses were performed by L.J. Schwarz; and atomic absorption analyses were performed by D.W. Golightly and P. Aruscavage; we greatly appreciate their considerable analytical effort. M. Mangan and D. Johnson helped with computer plots of the data. Reviews of this paper by D.A. Swanson and T.L. Wright have substantially improved the presentation of our results.

METHODS OF STUDY

We sampled and described the succession of flows in the Uwekahuna Bluff section (fig. 13.3) in sequence, starting immediately below the Uwekahuna triangulation station on the caldera

rim. Each flow unit was marked with a small aluminum tag bearing the appropriate unit number so that our sampling sites could be precisely revisited. We followed an existing trail near the top of the section down to about unit 12, below which we diverted to the north rim margin of a prominent talus cone (fig. 13.3) for the remainder of the

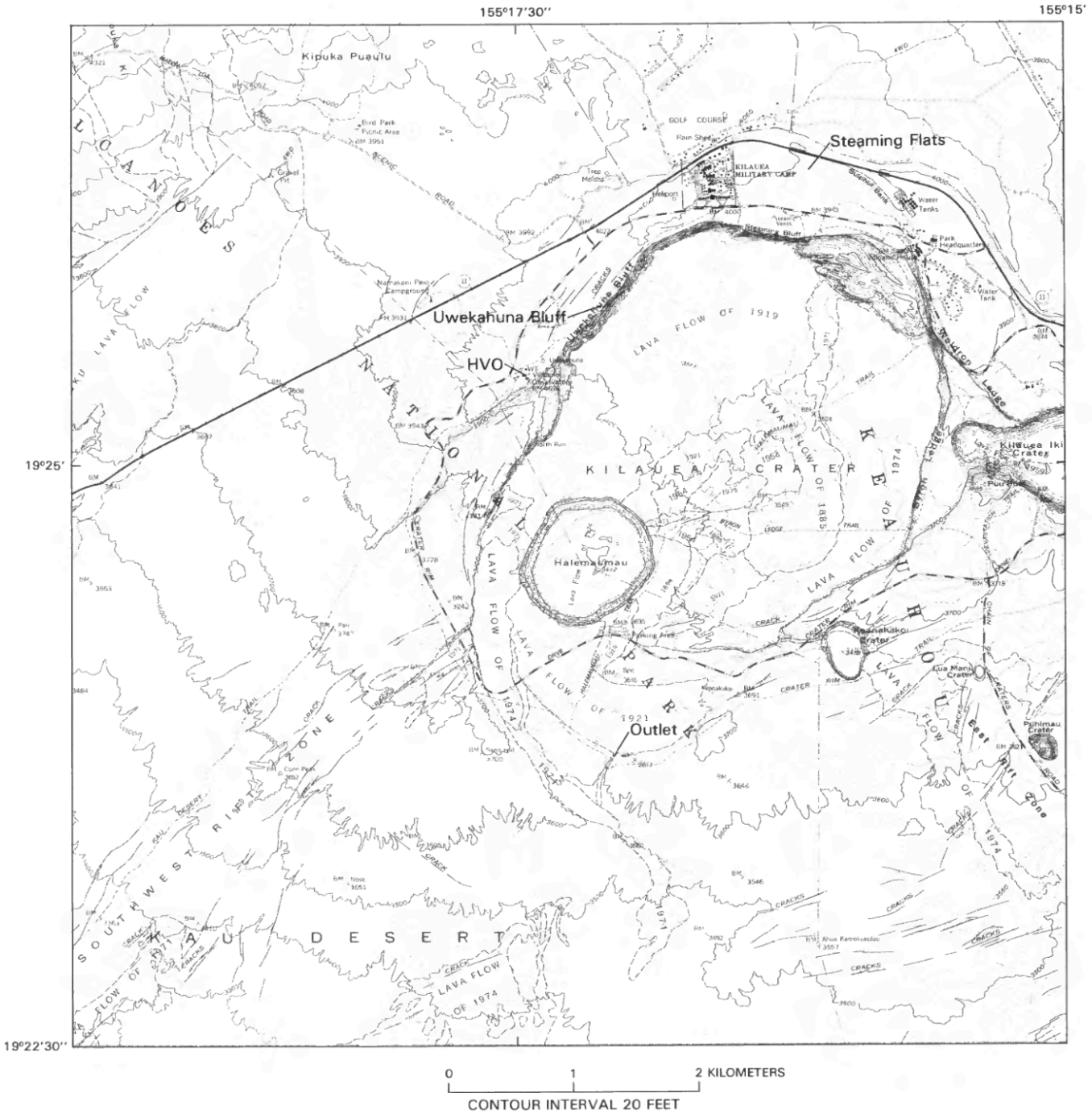


FIGURE 13.2.—Summit area of Kilauea, showing the location of segments of caldera wall examined in this study. Modified from U.S. Geological Survey Kilauea Crater 7.5-minute topographic map, 1981.

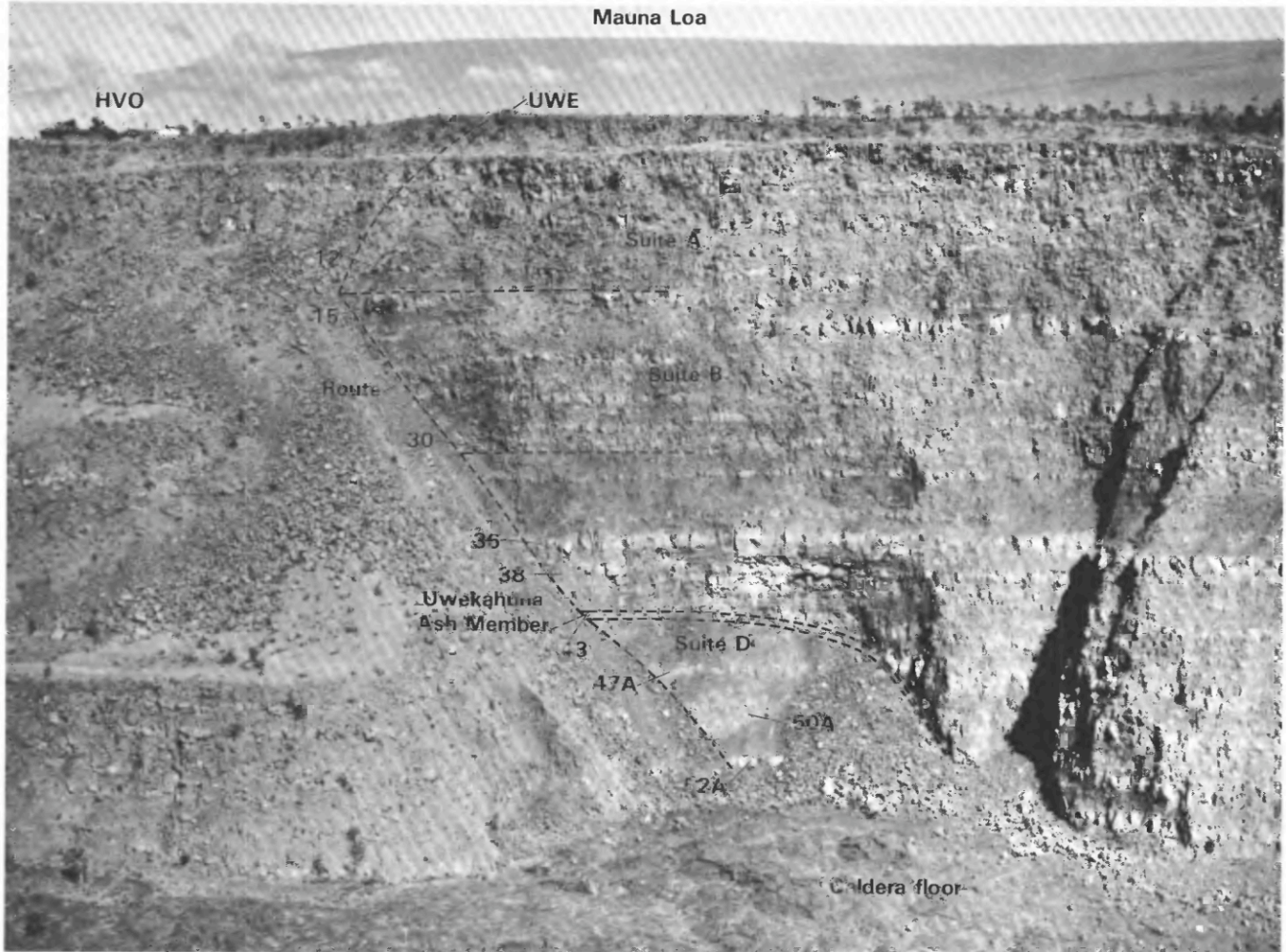


FIGURE 13.3.—Stratigraphic section exposed at Uwekahuna Bluff, with summit of Mauna Loa in distant background. Boundaries of lava suites A–D and position of the Uwekahuna Ash Member of the Puna Basalt are indicated. Selected units are labeled by number. Sampling route is shown by diagonal dashed line descending from Uwekahuna triangulation tower (UWE). HVO, Hawaiian Volcano Observatory. Height of cliff, from unit 52A up to rim, is 135 m.

section. After our sampling of the section in 1980, an earthquake in 1983 triggered rockfalls that buried the lower 50 m of the section, including all units below unit 38 (fig. 13.3).

Field criteria used to delineate lava flows and to distinguish between flows and sills include contact relations, particularly evidence for crosscutting and deformation of host rocks, and the textures of the top and bottom surfaces of a unit. Other features such as color, texture, mineralogy, and vesicle abundance and distribution, were occasionally helpful in tracing a flow unit. When viewed from a distance, the section appeared to have light-colored sills similar to the Uwekahuna laccolith. However, close examination of these suspected sills invariably revealed contact relationships that indicated an extrusive origin. We attempted to subdivide the Uwekahuna Bluff section as thoroughly as possible on the basis of field observations, while recognizing that petrologic considerations might eventually lead us to combine similar flow units into more generalized groups of flows.

The Uwekahuna Bluff section measured by Macdonald (Stearns and Macdonald, 1946, p. 193–194) differs from ours in detail, perhaps owing to different criteria used to distinguish flow units or to a different path selected for descent to the caldera floor.

FIELD OBSERVATIONS

Major features of the lava flows in the Uwekahuna Bluff section are summarized in table 13.1. The stratigraphic section at Uwekahuna Bluff consists of at least 63 flow units and 2 thick tephra deposits. The section is capped by the mostly A.D. 1790 Keanakakoi Ash Member, interpreted as the product of a large phreatomagmatic eruption possibly accompanied by partial caldera collapse (Swanson and Christiansen, 1973; Christiansen, 1979). The basal part of the Uwekahuna Ash Member exposed near the bottom of the bluff section has been assigned an age of 2.1 ka on the basis of radiocarbon dating of material from an inferred correlative

TABLE 13.1.—Description of rock units from Uwekahuna Bluff section, Kilauea caldera, Hawaii

[n.d., not determined]

Unit	Thickness (meters)	MgO content (wt percent)	Field description
Keanakakoi Ash Member			
0	0.3–1.0	n.d.	Ash from eruption circa A.D. 1790.
Suite A flows			
1	0.6	6.6	Flow varying in thickness from 0.3 to 1.3 m; vesicular pahoehoe with sparse olivine phenocrysts; reddish, oxidized ropy surface.
2	.9	6.6	Vesicular pahoehoe flow with sparse olivine phenocrysts.
3	4.9	6.6	Massive blocky flow with vesicular top, dense interior, and olivine phenocrysts.
4	2.75	6.8	Vesicular, ropy lava flow with red, ropy top and bottom; well-layered vesicularity; lower 0.6 m of unit is massive, dense; top and bottom flow surfaces dip toward caldera.
5	1.2	6.4	Vesicular, ropy lava flow; no layering of vesicles; similar to unit 4; flow contacts dip toward caldera.
6	4.25	6.7	Vesicular lava flow; top of flow is undulating and shows zones of vesicularity about 0.6 m wide; most of flow interior is dense.
7	.9	6.9	Vesicular flow that pinches out laterally; notably lenticular.
8	.6	6.8	Similar to flow 7.
9	1.5	7.0	Similar to flow 7.
10	3.35	6.7	Dense vesicular flow with rare zones 0.6–0.9 m thick, of dense nonvesicular material; lower 1.3 m is made of 1–3 reddish, oxidized, vesicular layers; base of unit is glassy.
11	4.1	7.3	Dense flow with rubbly, blocky aspect near top; in small gully, flow dips steeply toward crater, and measurement of true thickness is difficult.
12	5.0	6.3	Flow that dips toward caldera 27°–33°; rubble and talus cover in gully; large blocks and boulders cover this interval.
13	.3	6.6	Thin flow with glassy top and bottom.
14	.6	6.4	Thin flow with glassy top and bottom overlying reddish, highly oxidized zone.
Suite B flows			
15	1.7–10.5	7.0	Prominent red, oxidized layer with sharp upper contact; does not extend to south; may be faulted out or covered by rubble; may include several flows; oxidation occurs on fracture surfaces and in vesicles; flows dip toward caldera (maximum dip, 40°, average dip, 25°); reddish layers have a total thickness of 10.5 m; abundant loose blocks make it difficult to distinguish true bedrock.
16	.8	7.3	Distinct, thin flow unit with glassy top and bottom.
17	2.3	7.5	Light-gray rock with tiny olivine phenocrysts and irregular-shaped vesicles.
18	3.3	7.4	Massive flow with glassy top and bottom and dense zones or bands of nonvesicular material.
19	1.45	7.1	Flow with prominent irregular vesicles as large as 3 cm near top; rests on red, oxidized flow top that extends into cliff face to north.
20	.65	7.2	Thin flow, brownish gray and vesicular, that arches over an eye-shaped massive lens (tumulus?) and is overlain by prominent red, oxidized flow top.
21	2.5	7.4	Massive lens; thins rapidly to north.
22	.8	6.7	Unit composed of four thin, glassy vesicular flows with glassy tops.
23	.9–1.5	6.9	Unit of varying thickness, perhaps multiple flow units; highly vesicular with glassy flow tops and bottoms; thickens to north.
24	1.4	7.7	Vesicular flow with glassy top and red, oxidized glassy bottom; surface dips toward caldera.
25	2.1	8.0	Lens-like massive flow that thickens toward gully to south; may be an inflated pahoehoe flow.
26	4.4	7.8	Massive lens(?) of lava between two red, oxidized, vesicular flow contacts; open vugs as large as 1 cm; pipe vesicles in lower 2 m of flow.
27	4.3	7.0	Several thin (less than 1 m) red flows; highly vesicular; flow contacts dip 37°–39° and strike N. 35° E; this unit may be a tumulus.
28	2.4	7.5	Brown flow with irregular vesicles as large as 2 cm near top and dense interior with well-developed pipe vesicles; no coarse-grained zones; vesicles throughout; from a distance this unit may appear to be intrusive; to south this unit dips into gully; to north unit appears to thicken but is in cliff face and not accessible for measurement.
29	2.1	7.3	Similar in appearance to unit 28; massive, vesicular, brown, with glassy vesicular top; note 5 paleomagnetic drill holes 8X080 to 8X084; unit has prominent red, oxidized top and bottom surfaces that dip 21°–24° towards caldera and strike N. 38° E; this unit may be a tumulus.
30	1.9	7.4	Massive flow that thickens to 3.1 m in a 5-m lateral distance; vesicular throughout and highly fractured; brown-red color; a single flow with nearly horizontal top; to north along the cliff face unit appears more dense.
Suite C flows			
31	2.3	17.6	Package of thin, collapsed, shelly pahoehoe flows with excellent continuity to the north; highly vesicular with some ropy surfaces; individual flows from 4–10 cm in thickness; portions of unit contain abundant olivine phenocrysts (20 percent) as large as 5 mm.
32	1.5	18.1	Dense lava flow with obvious northward continuity and abundant olivine; paleomagnetic drill holes 8X075–8X079.
33	6.9	17.2	Prominent unit of numerous thin flows, probably collapsed shelly pahoehoe; flows highly vesicular, reddish, oxidized material, very friable; abundant olivine; flows dip about 5° away from caldera.
34	1.5	14.5	Prominent thin, dense, olivine-bearing lava flow, moderately vesicular; paleomagnetic drill holes 8X070–8X074; unit extends to north along cliff face.
35	2.5	13.7	Thin flows of collapsed shelly pahoehoe with prominent olivine phenocrysts (5–10 percent); unit dips 22° toward caldera.
36	3.3	13.2	Massive gray flow unit with lateral continuity to north; vesicular with prominent curving fractures; paleomagnetic drill holes 8X065–8X069; contains less olivine (up to 5 percent phenocrysts as large as 3 mm) than overlying units.
37	3.0	17.3	Gray-brown massive flow unit with large vesicles near top and dense interior; dips 10° toward caldera; poor lateral continuity, may be a lens; paleomagnetic drill holes 8X060–8X064.
38	2.4	9.0	Flow that interfingers with unit 37 to north, where units become difficult to distinguish; both have red, oxidized tops.
39	2.3	14.5	Unit composed of several thin horizontal layers 0.2–0.3 m thick; abundant (10 percent) olivine phenocrysts as large as 4 mm; paleomagnetic drill holes 1D070–1D075.
40	3.0	10.1	Massive, vesicular unit that becomes indistinct to north; contains abundant olivine (5 percent) as large as 2 mm but mostly less than 1 mm.
41	3.1	14.0	Vesicular unit that looks like aa flow, jumble of thin flows, and rubble; lower contact is red surface; contact with overlying flow is indistinct; contains abundant (5–10 percent) olivine as large as 3 mm.
42	1.3	19.7	Dense, vesicular flow above Uwekahuna Ash Member; paleomagnetic drill holes 1D076–1D083; abundant (10–15 percent) olivine phenocrysts with some lenses and pods containing as much as 50 percent olivine.

TABLE 13.1.—Description of rock units from Uwekahuna Bluff section, Kilauea caldera, Hawaii—Continued

Unit	Thickness (meters)	MgO content (wt percent)	Field description
Beneath unit 42			
43	1.5–2.2	6.5–9.7	Uwekahuna Ash Member.
Flows of suite C ponded against Uwekahuna Ash Member			
44	3.6	9.2	Upper 0.9 m, red rubble and vesicular flow with pipe vesicles; middle 1.2 m, massive flow with large, irregular vesicles; lower 1.5 m, dense, massive flow unit with finger-shaped gas vesicles.
45	7.1	13.0	Thick, massive unit overlain by 0.2–0.6 m, of reddish rubble; unit contains trains of vesicles in middle 1.5–2 m; olivine phenocrysts as large as 5 mm locally make up 10–15 percent of rock; obvious lateral continuity to north; flow has shattered or fractured appearance; bottom of unit rests on red, rubbly oxidized flow top.
46	1.8	13.3	Red, vesicular, blocky flows; several lobes of one or more flows, each with a well-preserved black glassy surface; fractured, with abundant olivine.
47	1.3	13.0	Gray-green massive flow with large irregular vesicles; olivine phenocrysts as large as 7 mm make up about 15 percent of rock; lower contact is glassy top of underlying flow unit 48.
48	3.2	9.8	Gray-green vesicular massive flow with abundant olivine as large as 3 mm.
49	.6	10.4	Olivine-rich (phenocrysts as large as 2 mm) pahoehoe flow overlying an aa flow.
50	2.7	10.1	Aa flow; top 1.5 m is rubble overlying dense interior; white sublimates on surface of blocks in rubble.
51	2.0	7.5	Dense flow overlying ash; contains portions of what may be foundered crust.
Uwekahuna Ash Member beneath unit 51			
---	4.8	---	Uwekahuna Ash Member here is 1.4 m thick; base of ash covered by 3.4 m of talus extending down to 1919 flows on caldera floor.
Suite D flows			
44A	0.6	n.d.	Scoriaceous rubble; possibly an aa flow top or scoria from nearby vent.
45A	2.4	n.d.	Massive, non-porphyrific, vesicular lava flow; lower 1.5 m forms prominent bench.
46A	1.6	n.d.	Mantled rubble, possibly infiltrated by tephra from unit 43; lower contact indistinct and highly oxidized, with some smooth, glassy (pahoehoe?) surfaces.
47A	2.4	7.1	Prominent massive flow clearly visible in fig. 13.3; fine-grained and vesicular, with weathered surface that is light colored; two paleomagnetic drill holes 1.2 m from lower contact, others may be covered by talus from the November 1975 earthquake; sample from dense lower portion of flow near paleomagnetic holes.
48A	4.2	n.d.	Rubble-covered flow; massive and vesicular; interior mostly covered by talus and ash from above, but appears to be dense and blocky; two paleomagnetic drill holes in lower portion of unit may be in an erratic boulder.
49A	1.8	n.d.	Massive, vesicular lava flow with buff weathered surface; flinty or glassy surface at top; unit contains eight paleomagnetic drill holes about 20 cm from lower contact.
50A	2.5	7.4	Massive flow unit with both vesicular and dense portions; dark gray in fresh outcrop, but buff on weathered surface; sampled near base of flow.
51A	4.2	n.d.	Flow 1.5 m below base of unit 50A; surface dips 32° toward caldera; most of interval is covered by rubble and talus overlying massive, buff unit 52A.
52A	2.2	7.8	Massive, dense unit at base of section; contains unusual texture, similar to that of foundered crust from Kilauea Iki drill holes—dense non-vesicular lenses interlayered with vesicular material; samples from middle of unit.
53A	4.1	n.d.	Talus-covered slope to caldera floor, which here consists of 1919 flow.

unit outside of the caldera (Lockwood and Rubin, 1986). Based on the wider dispersal of the Uwekahuna Ash Member, its eruptions were probably more violent than eruption of the Keanakakoi (Dzurisin and Casadevall, 1986).

Flows in the Uwekahuna Bluff section can be grouped into four suites differing in hand-specimen mineralogy and field occurrence (fig. 13.3). Suite A (units 1–14), at the top of the section, includes numerous thin lenticular pahoehoe flows containing small (less than 5 mm) plagioclase laths and rare olivine phenocrysts. A few thicker and more massive flows occur in this suite, but these usually lack the lateral persistence of similar massive flows lower in the section.

Suite B (units 15–30) consists of flows that contain rare phenocrysts of olivine and plagioclase. The glassy upper surface of flow 15, the youngest in suite B, is strongly weathered and pale yellow to red-brown. The texture of this surface is preserved, and no soil was found on it. This weathered surface is the only physical evidence we discovered for a significant time break within the Uwekahuna Bluff section; it correlates with the change from the mostly aphyric flows of suite B to the porphyritic flows of suite A.

Suite C (units 31–42 and 44–51; unit 43 is the Uwekahuna Ash Member) contains flows having abundant olivine phenocrysts and little or no plagioclase visible in hand specimen. The olivine

content in individual flows varies greatly and probably reflects crystal settling during flow (Fuller, 1939). We generally selected only one sample from each flow, and this is insufficient to characterize the olivine content of the entire flow. Several units consist of packages of thin (a few centimeters thick) highly vesicular layers interpreted as near-vent shelly pahoehoe flows that collapsed because of degassing and the weight of overlying flows (Swanson, 1973). A few units (for example, unit 36) are more massive and have dense interiors. These usually have appreciable lateral continuity and can be traced northward in the wall for as much as 2 km.

The Uwekahuna Ash Member (unit 43) underlies suite C. Along the south side of Uwekahuna Bluff, the ash directly underlies unit 42, about 35 m above the caldera floor (fig. 13.3). Farther north, the ash mantles an old northeast-facing slope and drops to within a few meters of the caldera floor (fig. 13.3). Ponded against this slope and overlying the ash are olivine-rich aa and pahoehoe lava flows (units 44–51), which petrographically and chemically resemble units 31–42.

Suite D (units 44A–52A) contains fairly massive and sparsely vesicular aphyric flows beneath the Uwekahuna Ash Member. Most are poorly exposed because of mantling by talus and ash from above. The near absence of olivine phenocrysts makes these flows petrographically distinct from those of suite C. Flows of suite D are

exposed in a 30-m-thick section that is cut off by a northeast-facing slope mantled by the Uwekahuna Ash Member and buried by the flows of suite C (fig. 13.3). North of Uwekahuna Bluff, the ash is essentially horizontal and extends for more than 1.5 km at a constant level above the caldera floor (Powers, 1948), which level corresponds to the lower elevation of the ash in the bluff section. The horizontal ash layer probably covered a broad, relatively flat surface, similar to that of the present caldera floor.

PETROGRAPHY

We examined 57 thin sections of rocks from Uwekahuna Bluff. Nearly all samples contain olivine phenocrysts in a holohyaline to holocrystalline groundmass. Most groundmass textures are intersertal, with brown glass between microlites. Intergranular texture is most common in the dense flow interiors, particularly in those from picritic units 44–51. Crystallinity ranges from about 25 to 85 percent. In the more crystalline samples, the groundmass consists of clinopyroxene and plagioclase in overlapping or felted microlites too small for individual crystals to be recognized. Most samples contain dark brown glass and scattered small anhedral opaque grains. Olivine is present as euhedral to subhedral phenocrysts that range in shape from stout and prismatic to elongate and lathlike. In most flows, a few olivine crystals occur in the microcrystalline groundmass. The olivine microlites and phenocrysts are in general partly resorbed and corroded. Clinopyroxene and plagioclase occur as coarse granular aggregates of subhedral crystals in which pyroxene subophitically or ophitically encloses plagioclase, as rosettes or sprays of clinopyroxene and plagioclase, and less commonly as individual phenocrysts and microlites.

Modal abundances for thin sections from 21 flows were determined by standard point-count methods (fig. 13.4). Microlites (0.05–1 mm) of plagioclase, clinopyroxene, and olivine; phenocrysts (greater than 1 mm) of plagioclase, clinopyroxene, and olivine; groundmass (microlites less than 0.05 mm); and vesicles were counted. Hypersthene was looked for but not found. Flows of suite C form a distinct cluster because of their high olivine content. Flows of suites B and D contain only sparse olivine and plagioclase, and flows of suite A are similar to the aphyric lavas except in their greater abundance of plagioclase.

CHEMISTRY

The basalt lavas of Uwekahuna Bluff are olivine tholeiite similar to other Kilauea summit flows (Macdonald, 1949; Wright, 1971; Wright and Tilling, 1980). Units 1–51 and 47A, 50A, and 52A were analyzed for major-element composition by rapid rock-analytical methods (Shapiro, 1975) and for trace-element and rare-earth-element compositions by instrumental neutron-activation (Baedecker, 1979) and atomic-absorption techniques (table 13.2). Precisions for major-element oxides (variation in percent of reported weight percent value) in rocks of basaltic composition are as follows: SiO₂ (0.3), Al₂O₃ (0.2), CaO (0.2), MgO (0.1), Na₂O (0.1), K₂O (0.1), Fe total (0.1), TiO₂ (0.05), P₂O₅ (0.04), MnO

(0.04). Error limits (variation in percent of reported ppm value) for trace-element analyses for one standard deviation (one sigma) are as follows: Ba (10–20), Co (1), Cr (1), Hf (2), Rb (25–30), Ta (3), Th (6–12), Zn (2), Zr (10), Sc (1), La (1–2), Ce (2), Nd (7–17), Sm (1), Eu (1), Gd (8–25), Tb (2–3), Tm (5–15), Yb (3), Lu (3). For Cu, Co, and Ni values determined by atomic absorption methods, uncertainties are ± 2 percent of reported ppm value. To facilitate comparison of chemical data, we have recalculated all analyses from table 13.2 on a dry-weight basis after converting iron to FeO_t (FeO_t = FeO + 0.9Fe₂O₃). The recalculated analyses are plotted on MgO variation diagrams (fig. 13.5), following Powers (1955) and Wright (1971, 1974).

MAJOR-ELEMENT CHEMISTRY

The major-element compositions of units 1–30 (suites A and B) and 47A, 50A, and 52A (suite D) are broadly similar (fig. 13.5A) and vary only slightly with stratigraphic position (fig. 13.6A). The MgO contents in all these units lie between 6.4 and 8.0 weight percent (table 13.2). Flow units 31 through 51 (suite C), however, contain various amounts of olivine, and their MgO contents range from 7.5 to 19.7 weight percent. The chemistries of units 31–51 show considerable variation with stratigraphic position (fig. 13.6A) because of differing olivine contents within each picritic flow. This wide range in olivine content for the picritic flows of suite C facilitates precise calculation of olivine-control lines by linear least-squares regression. This procedure yields equations of the form $y = ax + b$, where y is the major oxide or element, x is the MgO content, a is the slope, and b is the y intercept value at MgO = 0 weight percent (table 13.3). Most oxides correlate negatively with MgO (fig. 13.5A), indicating the diluting effect of increasing olivine content on elements that do not enter the olivine crystal structure.

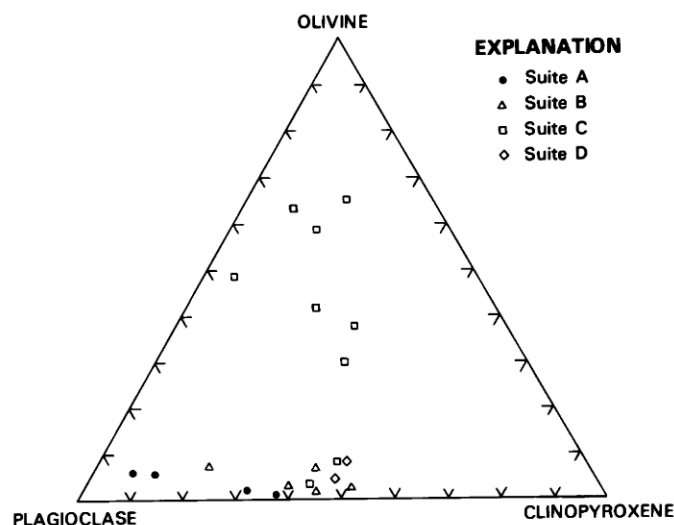


FIGURE 13.4.—Ternary diagram (clinopyroxene-olivine-plagioclase) derived from volumetric modal analyses (1,000 points per thin section) of 21 flows from Uwekahuna Bluff section.

TABLE 13.2.—Chemical analyses of Uwekahuna Bluff samples

[Values for oxides in weight percent; values for trace elements in parts per million. Symbols P, X, O, A, and U used to distinguish lava suites A–D and Uwekahuna Ash Member, respectively, in figs. 13.4–13.6 and 13.10. INAA, neutron-activation analysis; AA, atomic-absorption analysis; n.d., not determined; <, less than]

Sample symbol	UWE-1 P	UWE-2 P	UWE-3 P	UWE-4 P	UWE-5 P	UWE-6 P	UWE-7 P	UWE-8 P	UWE-9 P	UWE-10 P	UWE-11 P	UWE-12 P
SiO ₂	50.8	51.1	51.0	50.4	51.6	51.1	51.2	51.2	51.3	50.8	50.4	51.3
Al ₂ O ₃	14.0	14.0	13.8	13.9	13.8	13.8	13.7	13.6	13.9	13.8	13.6	13.8
Fe ₂ O ₃	2.5	5.7	2.9	6.7	5.3	5.2	6.6	4.3	4.1	4.5	3.2	6.7
FeO	8.9	5.9	9.1	5.8	7.4	7.2	5.6	7.5	7.7	8.0	8.4	5.7
MgO	6.6	6.6	6.6	6.8	6.4	6.7	6.9	6.8	7.0	6.7	7.3	6.3
CaO	10.5	10.7	10.6	10.5	10.6	10.7	10.7	10.7	10.5	10.7	11.2	10.7
Na ₂ O	2.5	2.3	2.4	2.4	2.5	2.4	2.4	2.4	2.4	2.5	2.3	2.5
K ₂ O	.47	.44	.47	.46	.46	.47	.44	.44	.44	.45	.42	.42
H ₂ O	.16	.21	.16	.18	.03	.30	.15	.10	.11	.17	.12	.29
TiO ₂	2.6	2.5	2.6	2.5	2.6	2.6	2.4	2.6	2.4	2.5	2.3	2.6
P ₂ O ₅	.31	.32	.32	.31	.32	.30	.29	.31	.30	.31	.29	.32
MnO	.22	.16	.18	.20	.18	.17	.17	.17	.18	.17	.16	.18
Ba	152	104	135	144	106	139	132	111	104	116	105	124
Co (INAA)	43	43	43	42	43	42	44	44	43	43	44	43
Co (AA)	44	44	44	46	42	44	43	46	44	42	42	44
Cr	353	336	309	338	313	327	366	331	351	313	354	235
Ni	96	100	93	91	80	91	110	98	100	87	93	82
Cu	130	120	99	130	130	95	120	130	130	120	92	140
Hf	4.06	3.93	4.05	3.85	4.13	4.00	3.85	4.02	3.92	4.00	3.57	4.05
Rb	<8	<20	16	10	9	12	15	13	13	14	<20	8
Ta	.94	.96	.95	.86	.97	.92	.88	.86	.81	.91	.83	.85
Th	.98	.84	.94	.88	.90	.83	.92	.78	.90	.89	.82	.83
U	<0.3	<0.3	<0.3	<0.3	.5	<0.3	<0.3	<0.3	<0.3	<0.3	<0.3	<0.4
Zn	112	108	111	105	118	111	108	113	110	110	109	116
Zr	152	164	181	158	152	159	138	159	151	182	145	117
Sc	31.0	31.0	30.7	30.8	32.1	30.7	30.6	31.6	31.0	31.7	33.4	33.0
La	12.7	12.7	12.9	11.9	12.8	11.8	11.7	11.8	11.6	11.8	10.8	10.9
Ce	31.6	29.9	30.3	28.5	31.3	29.5	29.5	28.9	28.2	29.7	26.5	27.8
Nd	19	21	20	12	22	20	20	21	22	24	20	18
Sm	5.83	5.76	5.89	5.66	6.09	5.66	5.68	5.81	5.57	5.80	5.28	5.80
Eu	1.93	1.89	1.91	1.83	2.04	1.88	1.90	1.92	1.89	1.92	1.78	1.93
Gd	5.8	6.6	5.8	6.1	7.4	6.4	5.8	6.4	7.1	6.9	5.9	6.0
Tb	1.02	.96	.98	.96	1.02	.95	.92	.96	.88	1.00	.88	1.01
Tm	.33	.17	.29	.29	.31	.35	.34	.39	.34	.39	.34	.41
Yb	2.22	2.25	2.18	2.26	2.48	2.17	2.25	2.31	2.09	2.18	2.08	2.48
Lu	.311	.299	.308	.301	.307	.290	.294	.309	.287	.319	.296	.340
Sample symbol	UWE-13 P	UWE-14 P	UWE-15-1 X	UWE-15-2 X	UWE-16 X	UWE-17 X	UWE-18 X	UWE-19 X	UWE-20 X	UWE-21 X	UWE-22 X	UWE-23 X
SiO ₂	51.4	50.8	51.6	51.2	50.3	51.1	51.7	50.8	50.4	51.3	50.4	50.7
Al ₂ O ₃	13.7	14.0	13.5	13.7	13.7	13.7	13.6	13.6	13.8	13.4	13.6	13.3
Fe ₂ O ₃	7.7	4.9	4.4	3.3	4.1	3.4	2.6	5.1	4.8	3.0	4.0	3.0
FeO	5.2	7.4	8.1	8.6	8.1	8.7	9.1	6.5	7.3	9.4	8.1	9.4
MgO	6.6	6.4	7.0	6.5	7.3	7.5	7.4	7.1	7.2	7.4	6.7	6.9
CaO	10.7	10.6	10.5	10.6	10.6	10.7	10.6	10.6	10.8	10.9	10.8	10.8
Na ₂ O	2.5	2.4	2.4	2.3	2.3	2.3	2.3	2.3	2.3	2.3	2.4	2.3
K ₂ O	.44	.43	.40	.40	.38	.38	.39	.38	.42	.42	.46	.47
H ₂ O	.06	.10	.05	.09	.14	.11	.07	.52	.29	.14	.25	.03
TiO ₂	2.6	2.5	2.6	2.5	2.4	2.4	2.4	2.4	2.4	2.5	2.7	2.7
P ₂ O ₅	.32	.30	.31	.28	.30	.30	.29	.28	.30	.30	.31	.30
MnO	.18	.18	.17	.17	.17	.16	.17	.17	.17	.17	.18	.17
Ba	90	97	<200	81	108	83	89	105	115	118	137	129
Co (INAA)	42	41	45	44	46	45	46	45	44	46	45	45
Co (AA)	42	42	44	44	46	48	46	48	44	46	44	48
Cr	266	235	415	287	354	386	354	351	344	316	252	265
Ni	91	84	100	96	100	110	110	100	110	110	80	87
Cu	140	140	120	110	120	100	110	120	120	98	140	120
Hf	3.74	3.76	3.68	3.81	3.67	3.48	3.66	3.67	3.59	4.00	4.05	4.06
Rb	12	9	<20	<20	<20	11	<20	<20	<20	12	11	<20
Ta	.80	.76	.74	.77	.74	.75	.77	.75	.79	.86	1.05	.99
Th	.73	.83	.66	.74	.74	.70	.77	.71	.69	.74	.91	.91
U	<0.3	0.30	<0.4	<0.4	<0.4	<0.3	<0.4	<0.4	<0.4	<0.4	0.30	<0.4
Zn	110	110	113	109	107	109	108	113	104	110	113	113
Zr	130	161	148	120	142	152	132	129	135	121	149	140
Sc	32.0	31.4	32.4	33.1	33.0	32.1	32.4	32.0	31.8	33.5	32.8	32.3
La	10.7	10.8	10.1	10.4	9.9	10.2	10.5	10.4	10.5	13.0	12.1	12.8
Ce	26.5	26.8	25.6	26.5	25.8	25.6	26.6	26.0	26.8	27.9	31.1	30.4
Nd	16	21	18	19	16	19	19	19	19	23	20	23
Sm	5.61	5.70	5.50	5.44	5.26	5.26	5.40	5.40	5.40	5.80	5.90	5.90
Eu	1.83	1.85	1.82	1.82	1.76	1.75	1.79	1.76	1.77	1.87	1.94	1.95
Gd	7.1	7.1	5.5	5.4	6.2	6.7	6.1	6.1	5.8	4.3	7.9	7.5
Tb	.93	.94	.97	.96	1.01	.91	.95	.93	.94	.98	.99	.95
Tm	.35	.39	.38	.35	.33	.32	.31	.26	.33	.30	.43	.29
Yb	2.25	2.34	2.35	2.12	2.19	2.17	2.27	2.10	2.03	2.42	2.37	2.20
Lu	.340	.319	.312	.299	.303	.301	.306	.301	.301	.300	.301	.322
Sample symbol	UWE-24 X	UWE-25-1 X	UWE-25-2 X	UWE-26 X	UWE-27 X	UWE-28 X	UWE-29 X	UWE-30-1 X	UWE-30-2 X	UWE-31 O	UWE-32 O	UWE-33 O
SiO ₂	50.0	50.7	50.6	50.9	50.6	50.5	50.8	50.5	50.8	47.6	47.7	47.7
Al ₂ O ₃	13.4	13.5	13.3	13.3	13.7	13.5	13.2	13.3	14.0	9.9	10.2	10.1
Fe ₂ O ₃	4.4	2.6	3.3	4.0	6.9	4.7	5.3	5.0	3.3	3.4	3.2	6.0
FeO	8.1	9.4	9.2	8.7	6.0	8.0	7.6	7.1	8.5	8.5	8.7	6.9
MgO	7.7	8.0	7.8	7.8	7.0	7.5	7.3	7.4	6.5	17.6	18.1	17.2
CaO	11.1	11.4	11.1	10.9	11.0	10.9	11.0	10.9	10.6	7.9	9.0	9.0
Na ₂ O	2.0	2.3	2.3	2.2	2.4	2.5	2.5	2.2	2.5	1.5	1.6	1.6

TABLE 13.2.—Chemical analyses of Uwekahuna Bluff samples—Continued

Sample symbol	UWE-1 P	UWE-2 P	UWE-3 P	UWE-4 P	UWE-5 P	UWE-6 P	UWE-7 P	UWE-8 P	UWE-9 P	UWE-10 P	UWE-11 P	UWE-12 P
K ₂ O	.45	.43	.43	.42	.44	.50	.47	.43	.45	.30	.29	.30
H ₂ O	.14	.08	.50	.07	.23	.24	.09	.22	.12	.41	.19	.28
TiO ₂	2.1	2.4	2.4	2.4	2.6	2.5	2.6	2.5	2.5	1.8	1.8	1.9
P ₂ O ₅	.29	.26	.28	.28	.29	.29	.31	.29	.31	.18	.21	.23
MnO	.20	.18	.17	.16	.18	.17	.18	.18	.17	.16	.15	.17
Ba	106	114	108	131	142	132	155	151	95	n.d.	140	96
Co (INAA)	46	48	47	48	44	45	46	45	43	n.d.	76	72
Co (AA)	49	49	48	49	46	46	44	44	44	n.d.	74	74
Cr	403	440	456	461	321	332	346	372	309	n.d.	1100	1040
Ni	110	120	120	130	89	96	100	110	89	n.d.	760	740
Cu	120	95	91	110	120	130	120	130	110	n.d.	90	96
Hf	3.83	3.57	3.61	3.69	3.90	3.97	3.86	3.74	4.01	n.d.	2.98	2.95
Rb	15	<20	<20	13	13	12	<20	<20	<10	n.d.	<20	14
Ia	.92	.82	.84	.94	1.01	.98	1.01	1.02	.85	n.d.	.72	.75
Th	.85	.88	.64	.88	.99	.84	.86	.85	.81	n.d.	.52	.60
U	<0.4	<0.4	<0.4	.16	<0.5	.27	.21	.24	.30	n.d.	<0.5	.27
Zn	111	110	109	107	111	109	114	109	108	n.d.	105	102
Zr	144	146	168	135	167	162	127	166	147	n.d.	131	103
Sc	31.5	32.8	32.7	32.7	32.0	31.6	32.5	33.0	31.4	n.d.	26.0	25.3
La	12.2	10.6	11.0	11.4	12.7	12.4	13.3	12.6	12.2	n.d.	8.9	9.29
Ce	28.0	26.1	26.6	27.4	30.7	30.5	30.6	30.5	29.7	n.d.	22.7	22.9
Nd	22	18	16	23	23	22	21	21	26	n.d.	18	15.8
Sm	5.84	5.30	5.40	5.50	6.10	5.80	6.00	5.85	6.00	n.d.	4.42	4.23
Eu	1.81	1.70	1.73	1.79	1.85	1.86	1.84	1.80	1.92	n.d.	1.38	1.37
Gd	6.7	5.6	6.4	5.2	5.2	6.6	5.7	5.9	7.2	n.d.	3.4	3.6
Tb	.99	.87	.87	.88	.94	.92	.97	.91	1.00	n.d.	.79	.65
Tm	.35	.35	.39	.32	.33	.31	.32	.33	.37	n.d.	.31	.213
Yb	2.03	2.02	2.11	2.09	2.19	2.05	2.07	2.00	2.47	n.d.	1.73	1.65
Lu	.299	.270	.280	.310	.313	.309	.34	.27	.317	n.d.	.26	.238
Sample symbol	UWE-34 O	UWE-35 O	UWE-36 O	UWE-37 O	UWE-38 O	UWE-39 O	UWE-40 O	UWE-41 O	UWE-42 O	UWE-43 U	UWE-44 O	UWE-45 O
SiO ₂	48.6	48.6	48.8	48.0	50.5	49.0	49.4	48.9	47.2	50.8	50.8	49.2
Al ₂ O ₃	11.2	11.4	11.6	10.0	13.2	10.8	12.4	11.6	9.4	13.2	13.0	10.7
Fe ₂ O ₃	5.4	8.1	4.8	3.0	4.8	4.0	5.8	5.8	3.3	3.1	4.0	3.3
FeO	6.8	4.6	7.4	9.3	6.5	8.8	7.9	6.4	9.6	8.0	7.6	9.7
MgO	14.5	13.7	13.2	17.3	9.0	14.5	10.1	14.0	19.7	9.5	9.2	13.0
CaO	9.6	9.5	10.0	8.4	10.5	8.9	10.5	9.5	8.3	10.2	10.9	8.8
Na ₂ O	1.7	1.8	1.9	1.7	2.2	1.8	2.0	2.0	1.5	1.9	2.2	2.0
K ₂ O	.30	.35	.39	.34	.41	.39	.43	.37	.26	.42	.42	.46
H ₂ O	.11	.19	.64	.18	.30	.27	.40	.15	.27	.27	.20	.24
TiO ₂	2.1	2.2	2.2	1.8	2.5	2.2	2.4	2.2	1.5	2.4	2.5	2.8
P ₂ O ₅	.23	.25	.26	.22	.29	.25	.31	.27	.17	.29	.29	.36
MnO	.19	.15	.18	.17	.17	.16	.16	.14	.18	.16	.16	.16
Ba	99	96	<100	<200	<200	<200	86	90	<200	107	81	120
Co (INAA)	65	62	63	76	48	71	53	62	85	50	45	64
Co (AA)	66	63	66	79	50	72	58	68	85	53	50	68
Cr	961	869	887	1090	602	987	687	861	1260	535	626	790
Ni	580	490	490	790	230	600	320	490	870	230	220	500
Cu	100	95	89	78	120	100	110	110	53	110	120	120
Hf	3.06	3.26	3.43	2.72	3.8	3.30	3.61	3.32	2.33	3.30	3.7	4.15
Rb	11	10	<30	13	18	<30	11	<30	<30	8	<30	13
Ia	.79	.81	.87	.64	.91	.87	.91	.86	.56	.85	.95	1.09
Th	.67	.70	.65	.51	.75	.65	.67	.60	.52	.82	.73	.70
U	<0.5	.35	<0.4	<0.5	.23	<0.3	<0.5	.33	<0.4	.40	.44	.31
Zn	104	106	112	108	119	107	109	109	108	103	100	122
Zr	104	103	140	<100	131	<200	148	178	120	154	136	152
Sc	27.1	27.2	27.7	24.6	31.2	27.3	29.6	27.5	24.2	28.1	30.1	28.3
La	9.88	10.2	11.0	8.3	11.6	10.3	11.5	10.6	7.0	11.7	12.4	12.9
Ce	24.1	24.8	26.6	21.1	27.6	25.6	27.0	24.9	18.3	26.6	28.3	30.4
Nd	16.9	17.7	22	13	24	16	19	18	11	21	18	23
Sm	4.50	4.72	5.13	4.11	5.44	4.81	5.31	5.00	3.47	5.56	5.59	5.93
Eu	1.50	1.53	1.65	1.37	1.81	1.55	1.70	1.56	1.16	1.62	1.76	1.83
Gd	3.8	3.6	6.2	4.8	6.7	5.5	6.5	5.3	4.1	6.0	6.4	6.0
Tb	.71	.72	.88	.62	.97	.77	.85	.84	.58	.80	.96	.96
Tm	.20	.241	.27	.22	.38	.27	.31	.29	.19	.40	.29	.32
Yb	1.76	1.83	1.93	1.56	2.24	1.76	2.13	1.85	1.45	2.02	2.23	2.24
Lu	.259	.265	.287	.238	.34	.25	.299	.27	.21	.310	.30	.319
Sample symbol	UWE-46 O	UWE-47 O	UWE-48 O	UWE-49 O	UWE-50 O	UWE-51 O	UWE-47A A	UWE-50A A	UWE-52A A			
SiO ₂	49.0	47.4	47.5	48.4	50.0	50.1	49.8	50.0	49.6			
Al ₂ O ₃	11.5	11.5	12.4	12.4	12.8	13.1	13.6	13.2	13.5			
Fe ₂ O ₃	3.9	3.7	2.4	5.0	2.7	2.4	3.0	3.0	3.4			
FeO	8.5	8.8	9.8	7.0	9.0	9.2	8.5	9.0	8.3			
MgO	13.3	13.0	9.8	10.4	10.1	7.5	7.1	7.4	7.8			
CaO	9.0	10.4	12.2	11.2	11.2	11.4	12.1	11.1	11.3			
Na ₂ O	1.9	2.0	2.3	2.2	2.1	2.2	2.2	2.3	2.3			
K ₂ O	.35	.37	.41	.42	.39	.44	.49	.50	.44			
H ₂ O	.82	.24	.30	.08	.19	.36	.54	.36	.52			
TiO ₂	2.3	2.2	2.6	2.5	2.3	2.6	2.7	2.6	2.6			
P ₂ O ₅	.25	.29	.22	.33	.26	.31	.31	.29	.29			
MnO	.18	.18	.20	.18	.18	.18	.18	.20	.18			
Ba	<200	<200	120	133	103	123	148	128	127			
Co (INAA)	68	61	51	52	54	45	44	44	45			
Co (AA)	75	67	56	58	60	52	48	50	50			
Cr	946	753	555	597	739	395	285	334	347			

TABLE 13.2.—Chemical analyses of Uwekahuna Bluff samples—Continued

Sample symbol	UWE-46 O	UWE-47 O	UWE-48 O	UWE-49 O	UWE-50 O	UWE-51 O	UWE-47A A	UWE-50A A	UWE-52A A
Ni	670	460	220	240	290	120	100	110	120
Cu	71	100	130	120	98	100	91	67	110
Hf	2.99	3.5	3.8	3.68	3.4	3.9	4.01	3.98	3.8
Rb	<30	<30	<30	14	<30	15	<30	14	<20
Ta	.70	.93	1.02	.94	.85	1.03	1.10	1.13	1.08
Th	.70	.73	.80	.78	.68	.86	.97	.98	.92
U	.28	<0.5	<0.5	.29	.32	<0.6	<0.5	.30	<0.6
Zn	108	106	113	113	101	121	106	115	112
Zr	102	<200	140	130	152	154	125	202	179
Sc	25.4	27.2	29.9	30.0	30.0	31.8	31.1	31.4	31.3
La	9.6	11.1	12.7	11.7	10.7	12.4	13.4	13.8	13.3
Ce	23.9	26.9	29.8	28.3	26.3	29.3	32.4	32.7	31.3
Nd	21	18	19	20	15	20	24	21	23
Sm	4.61	5.28	5.83	5.48	5.11	5.75	5.82	5.88	5.61
Eu	1.46	1.68	1.88	1.81	1.69	1.89	1.93	1.92	1.84
Gd	4.6	6.1	6.4	6.2	5.6	7.0	7.2	6.9	5.8
Tb	.72	.80	1.00	.90	.75	.91	.95	.91	.88
Tm	.29	.28	.33	.35	.28	.34	.32	.31	.27
Yb	1.80	2.06	2.24	2.19	1.89	2.25	2.19	2.17	2.05
Lu	.244	.27	.30	.297	.27	.34	.36	.304	.297

TABLE 13.3.—Olivine control lines

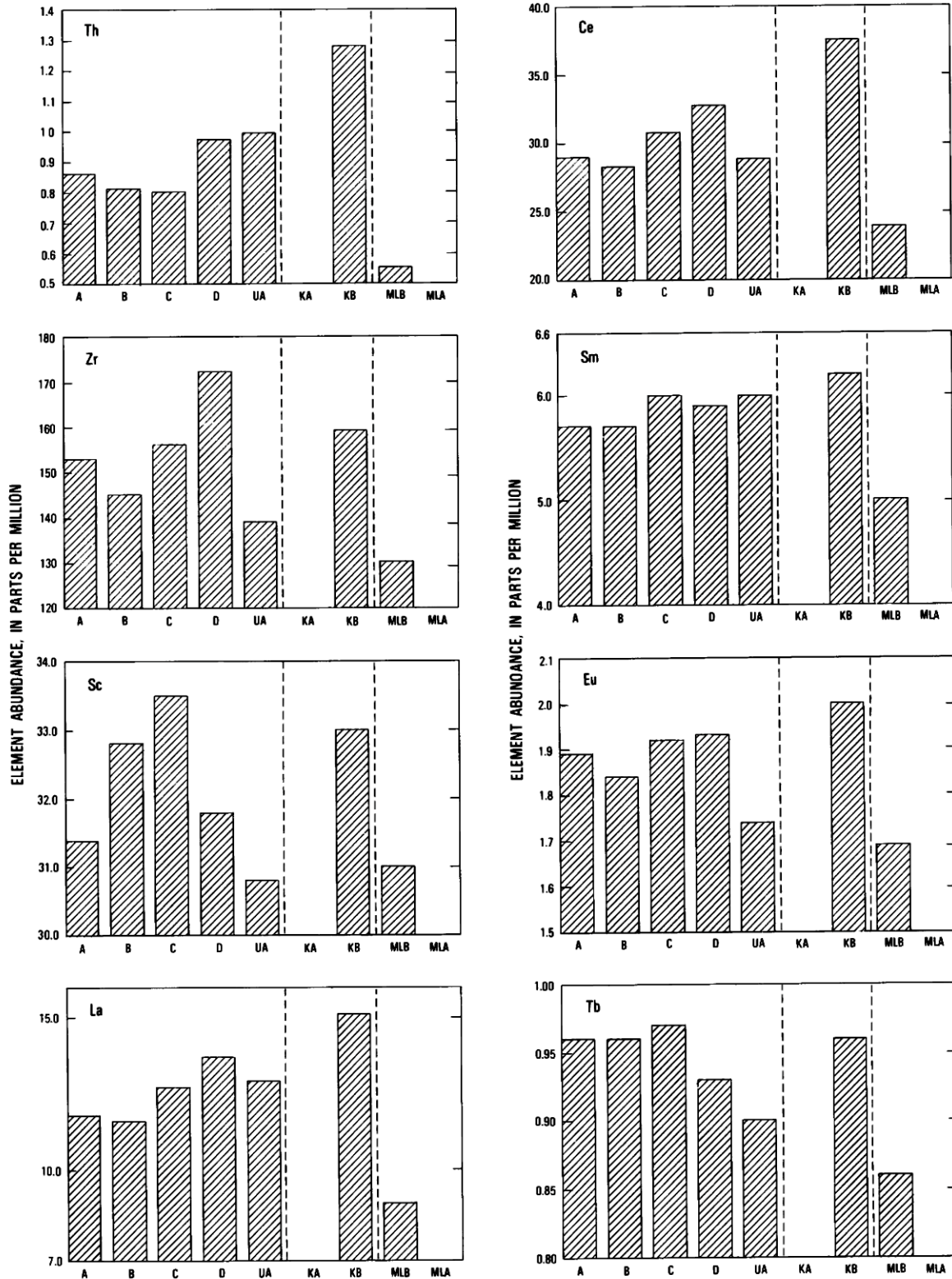
[Coefficients for equations of the form $y = ax + b$, where y is the major oxide or element, x is the MgO content, a is the slope, and b is the y intercept value at MgO = 0 weight percent. Values for oxides in weight percent; values for trace elements in parts per million; uncertainty is one standard deviation either side of the mean slope. Data for PHKILCAL (prehistoric Kilauea caldera and Hilina flows), KIL1959 (Kilauea Iki, 1959), HISTML (historic Mauna Loa), and PPPC (prehistoric pahoehoe picrite complex flows from Wright, 1971). FeO, total iron oxide = FeO + 0.9 Fe₂O₃; n.d., not determined]

Element	Suites A-D		Suite C		PPPC		PHKILCAL		KIL1959		HISTML	
	(a)	(b)	(a)	(b)	(a)	(b)	(a)	(b)	(a)	(b)	(a)	(b)
SiO ₂	-0.315 ± .028	52.842	-0.248 ± .064	51.828	-0.289 ± 0.023	52.894	-0.317 ± 0.021	53.327	-0.266 ± 0.005	51.922	-0.312 ± 0.010	54.260
Al ₂ O ₃	- .348 ± .012	16.036	- .336 ± .025	15.852	- .357 ± .010	16.643	- .354 ± .028	16.585	- .325 ± .008	15.943	- .338 ± .007	16.527
FeO	.027 ± .020	11.456	.071 ± .037	10.811	.068 ± .017	10.480	.081 ± .030	10.260	.035 ± .003	11.046	.025 ± .006	10.747
CaO	- .204 ± .027	12.298	- .306 ± .056	12.797	- .288 ± .017	12.184	- .266 ± .016	13.044	- .284 ± .010	12.674	- .263 ± .005	12.400
Na ₂ O	- .073 ± .005	2.852	- .070 ± .008	2.822	- .053 ± .007	2.691	- .065 ± .005	2.753	- .059 ± .002	2.705	- .059 ± .003	2.702
K ₂ O	- .013 ± .002	.524	- .015 ± .003	.556	- .014 ± .003	.561	- .012 ± .003	.497	- .015 ± .001	.658	- .006 ± .002	.409
TiO ₂	- .060 ± .008	2.946	- .086 ± .015	3.348	- .065 ± .006	2.906	- .057 ± .012	2.843	- .072 ± .003	3.263	- .045 ± .004	2.380
P ₂ O ₅	- .009 ± .001	.359	- .008 ± .003	.348	- .006 ± .001	.266	- .005 ± .001	.259	- .007 ± .001	.324	- .004 ± .001	.246
MnO	- .002 ± .001	.182	- .002 ± .002	.183	.000 ± .001	.164	n.d.	n.d.	n.d.	n.d.	n.d.	n.d.
Ba	-1.277 ± 1.505	126.440	.565 ± 2.649	100.346	n.d.	n.d.	n.d.	n.d.	n.d.	n.d.	n.d.	n.d.
Co (INAA)	3.047 ± .096	22.648	3.297 ± .253	19.006	n.d.	n.d.	n.d.	n.d.	n.d.	n.d.	n.d.	n.d.
Co (AA)	3.184 ± .144	23.350	2.772 ± .353	29.385	n.d.	n.d.	n.d.	n.d.	n.d.	n.d.	n.d.	n.d.
Cr	76.943 ± 3.049	-191.459	63.771 ± 6.067	2.147	n.d.	n.d.	n.d.	n.d.	n.d.	n.d.	n.d.	n.d.
Ni	63.766 ± 1.882	-349.095	65.268 ± 5.240	-368.050	n.d.	n.d.	n.d.	n.d.	n.d.	n.d.	n.d.	n.d.
Cu	-3.240 ± .858	139.767	-3.969 ± 1.398	151.439	n.d.	n.d.	n.d.	n.d.	n.d.	n.d.	n.d.	n.d.
Hf	- .094 ± .011	4.525	- .113 ± .025	4.831	n.d.	n.d.	n.d.	n.d.	n.d.	n.d.	n.d.	n.d.
Rb	.040 ± .202	12.028	- .289 ± .345	16.829	n.d.	n.d.	n.d.	n.d.	n.d.	n.d.	n.d.	n.d.
Ta	- .015 ± .006	1.013	- .032 ± .009	1.272	n.d.	n.d.	n.d.	n.d.	n.d.	n.d.	n.d.	n.d.
Th	- .027 ± .004	1.023	- .025 ± .005	1.001	n.d.	n.d.	n.d.	n.d.	n.d.	n.d.	n.d.	n.d.
U	.000 ± .010	.282	- .005 ± .012	.369	n.d.	n.d.	n.d.	n.d.	n.d.	n.d.	n.d.	n.d.
Zn	- .378 ± .239	113.205	- .700 ± .600	118.175	n.d.	n.d.	n.d.	n.d.	n.d.	n.d.	n.d.	n.d.
Zr	-3.090 ± 1.128	171.309	-3.137 ± 2.066	171.211	n.d.	n.d.	n.d.	n.d.	n.d.	n.d.	n.d.	n.d.
Sc	- .654 ± .052	36.464	- .635 ± .074	36.140	n.d.	n.d.	n.d.	n.d.	n.d.	n.d.	n.d.	n.d.
La	- .259 ± .057	13.718	- .409 ± .079	15.931	n.d.	n.d.	n.d.	n.d.	n.d.	n.d.	n.d.	n.d.
Ce	- .600 ± .110	33.117	- .800 ± .162	36.090	n.d.	n.d.	n.d.	n.d.	n.d.	n.d.	n.d.	n.d.
Nd	- .421 ± .150	23.420	- .578 ± .267	25.673	n.d.	n.d.	n.d.	n.d.	n.d.	n.d.	n.d.	n.d.
Sm	- .135 ± .015	6.669	- .170 ± .033	7.194	n.d.	n.d.	n.d.	n.d.	n.d.	n.d.	n.d.	n.d.
Eu	- .047 ± .004	2.189	- .056 ± .008	2.333	n.d.	n.d.	n.d.	n.d.	n.d.	n.d.	n.d.	n.d.
Gd	- .185 ± .054	7.549	- .291 ± .070	9.128	n.d.	n.d.	n.d.	n.d.	n.d.	n.d.	n.d.	n.d.
Tb	- .025 ± .003	1.129	- .029 ± .008	1.186	n.d.	n.d.	n.d.	n.d.	n.d.	n.d.	n.d.	n.d.
Tm	- .009 ± .003	.402	- .011 ± .004	.432	n.d.	n.d.	n.d.	n.d.	n.d.	n.d.	n.d.	n.d.
Yb	- .054 ± .007	2.595	- .068 ± .012	2.822	n.d.	n.d.	n.d.	n.d.	n.d.	n.d.	n.d.	n.d.
Lu	- .006 ± .001	.354	- .009 ± .002	.392	n.d.	n.d.	n.d.	n.d.	n.d.	n.d.	n.d.	n.d.

TRACE-ELEMENT CHEMISTRY AND RARE-EARTH-ELEMENT CHEMISTRY

Nearly all flows in the section were analyzed for a suite of 22 trace elements (table 13.2). Most of the trace elements show negative linear trends when plotted against MgO (fig. 13.5B; table 13.3), indicating that olivine abundance exerts the principal control on trace-element content. However, several trace elements correlate positively with MgO (table 13.3). Ni and Co, which resembles Ni in its behavior, are strongly partitioned from the melt into the olivine

crystal structure (Gunn, 1971; Hart and Davis, 1978). The positive correlation between Cr and MgO probably reflects the presence of inclusions of chrome spinel in olivine (Gunn, 1971). Our results for Cu differ from those of Gunn (1971), who found a significant positive correlation between MgO and Cu, probably indicating sulfide saturation in his samples. We found no correlation between Cu and MgO, and this may indicate varying levels of sulfur in the magmas supplying suite C flows (T.L. Wright, oral commun., 1985).



average from Wright (1971); KB, Kilauea average from Basaltic Volcanism Study Project (1981); MLB, Mauna Loa average from Basaltic Volcanism Study Project (1981); MLA, Mauna Loa average from Wright (1971). Vertical lines separate Uwekahuna Bluff data (left) from Kilauea averages (middle), and from Mauna Loa averages (right).

The rare-earth-element (REE) concentrations correlate negatively with MgO (fig. 13.5C), owing to the diluting effect of olivine crystals on the absolute concentrations of REE (Hanson, 1980). Chondrite-normalized REE data for selected flows from each suite show smooth curves with similar slopes (fig. 13.7A). In flows of suite

C, differences in the positions of the curves reflect the large range in olivine content, whereas flows of suites A, B, and D have a smaller range in REE abundances. The shapes and slopes of the curves for all flows within the Uwekahuna Bluff section are similar, suggesting that the parent magmas had a similar origin.

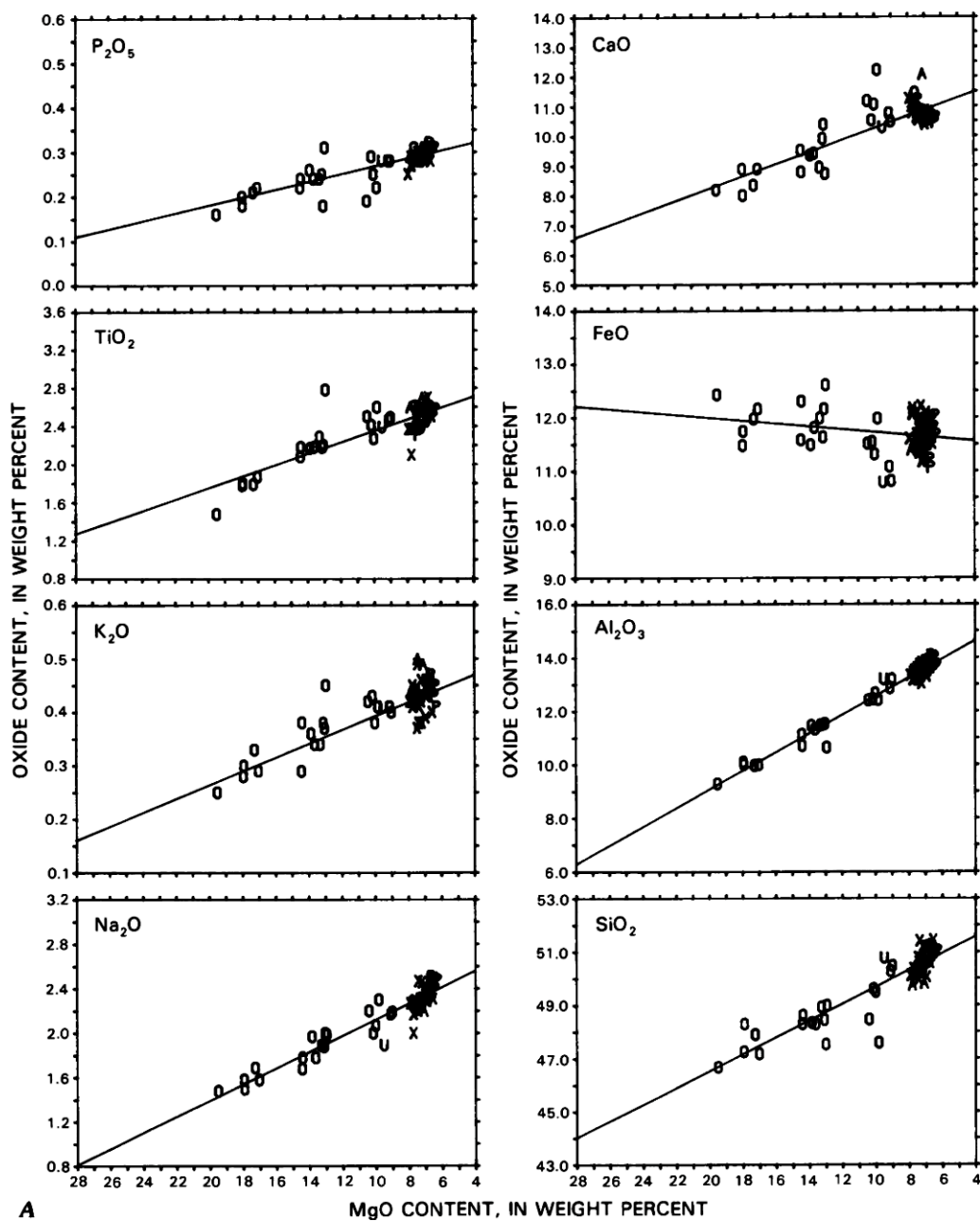


FIGURE 13.5.—MgO variation diagrams for flows of Uwekahuna Bluff section. Data symbols: P, flows of suite A, plagioclase porphyritic; X, flows of suite B, mostly aphyric; O, flows of suite C, olivine porphyritic; U, Uwekahuna Ash Member (unit 43); A, flows of suite D, aphyric. Lines are olivine-control lines for these data determined by linear least-squares regression. See table 13.3 for coefficients and figure 13.8 for comparison with olivine-control lines for other Kilauea lavas. **A**, Plots of major-element oxides versus MgO. **B**, Plots of trace elements versus MgO. **C**, Plots of rare-earth elements versus MgO.

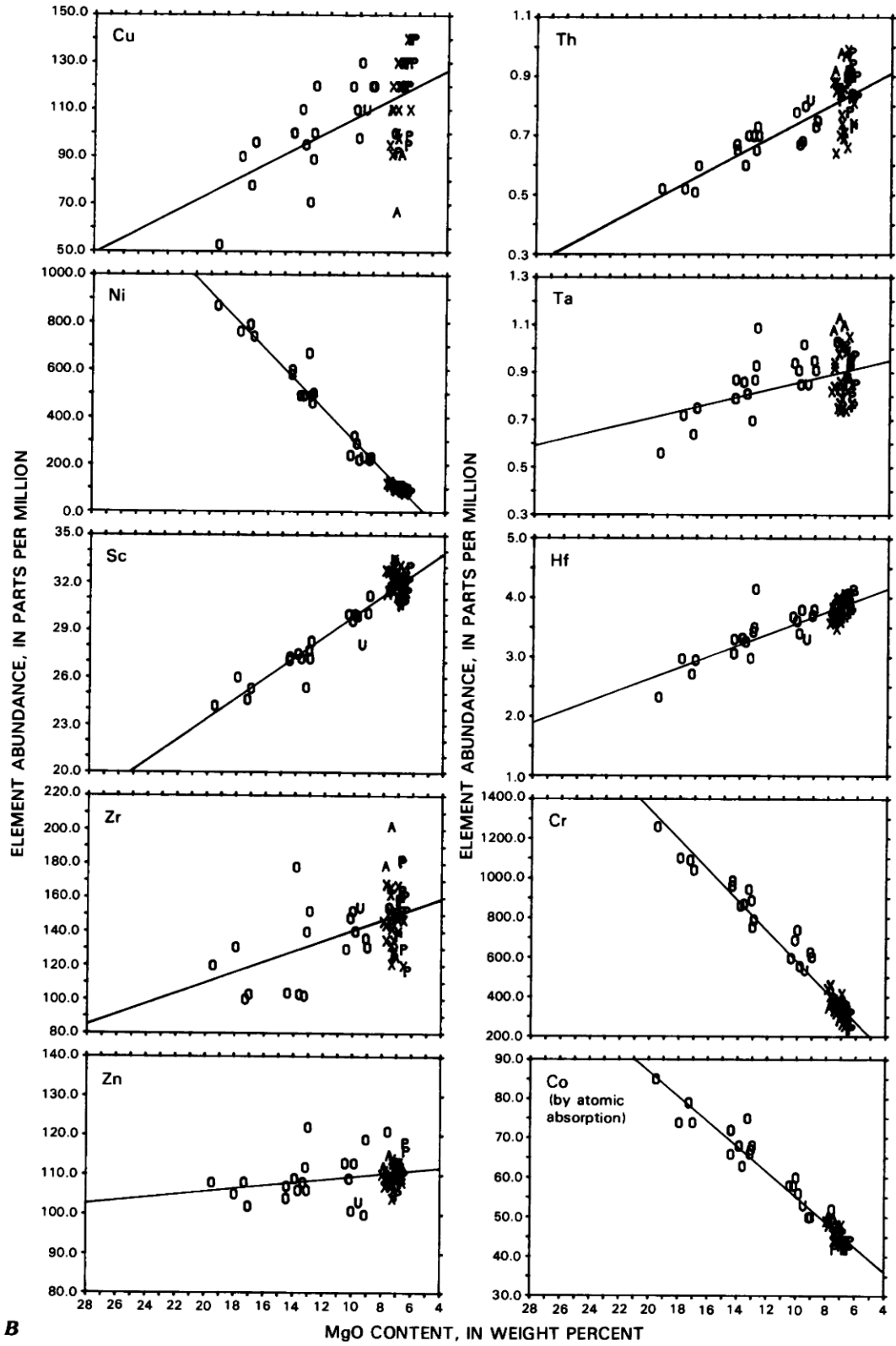
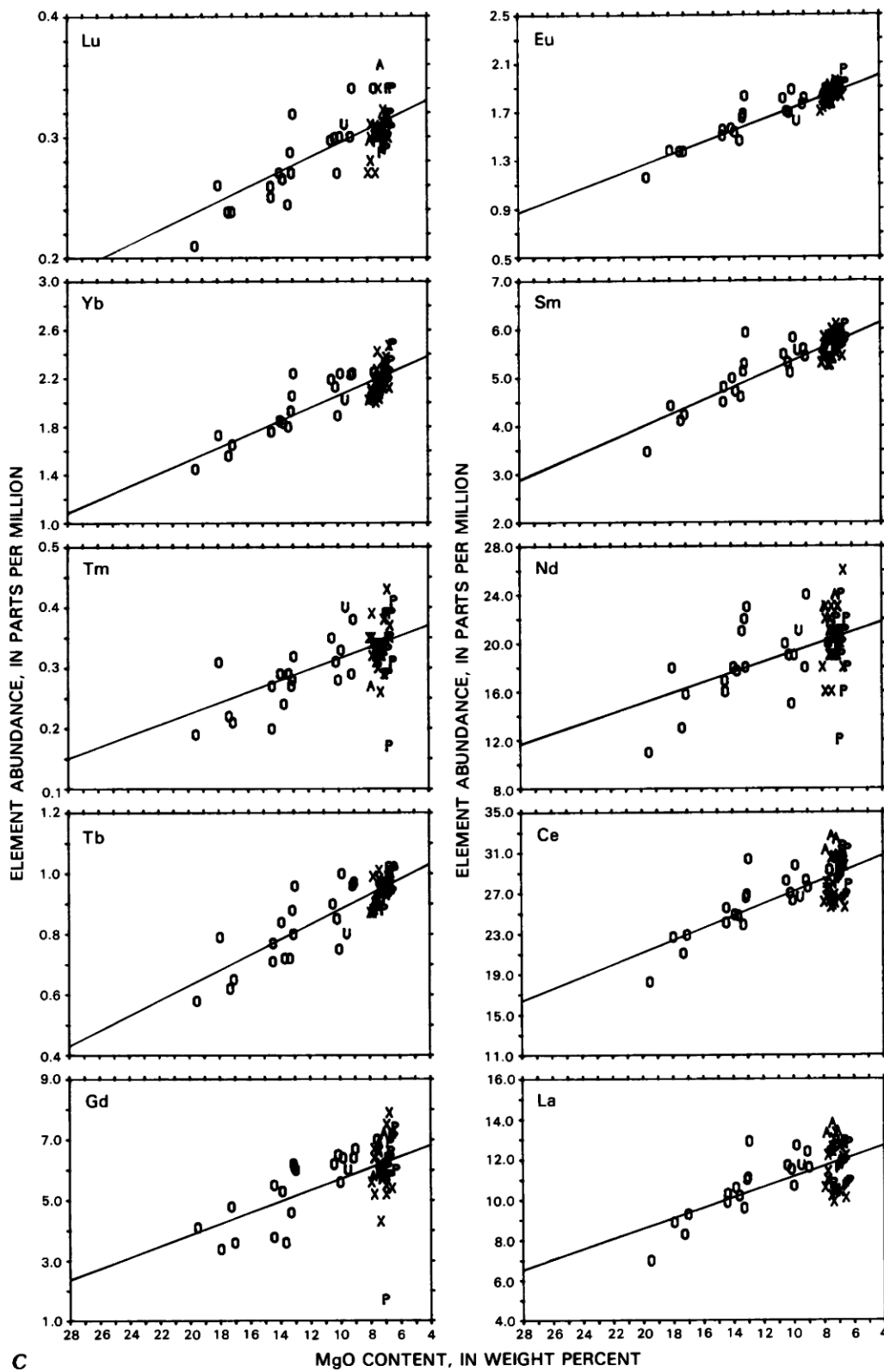


FIGURE 13.5.—Continued.



C

FIGURE 13.5.—Continued.

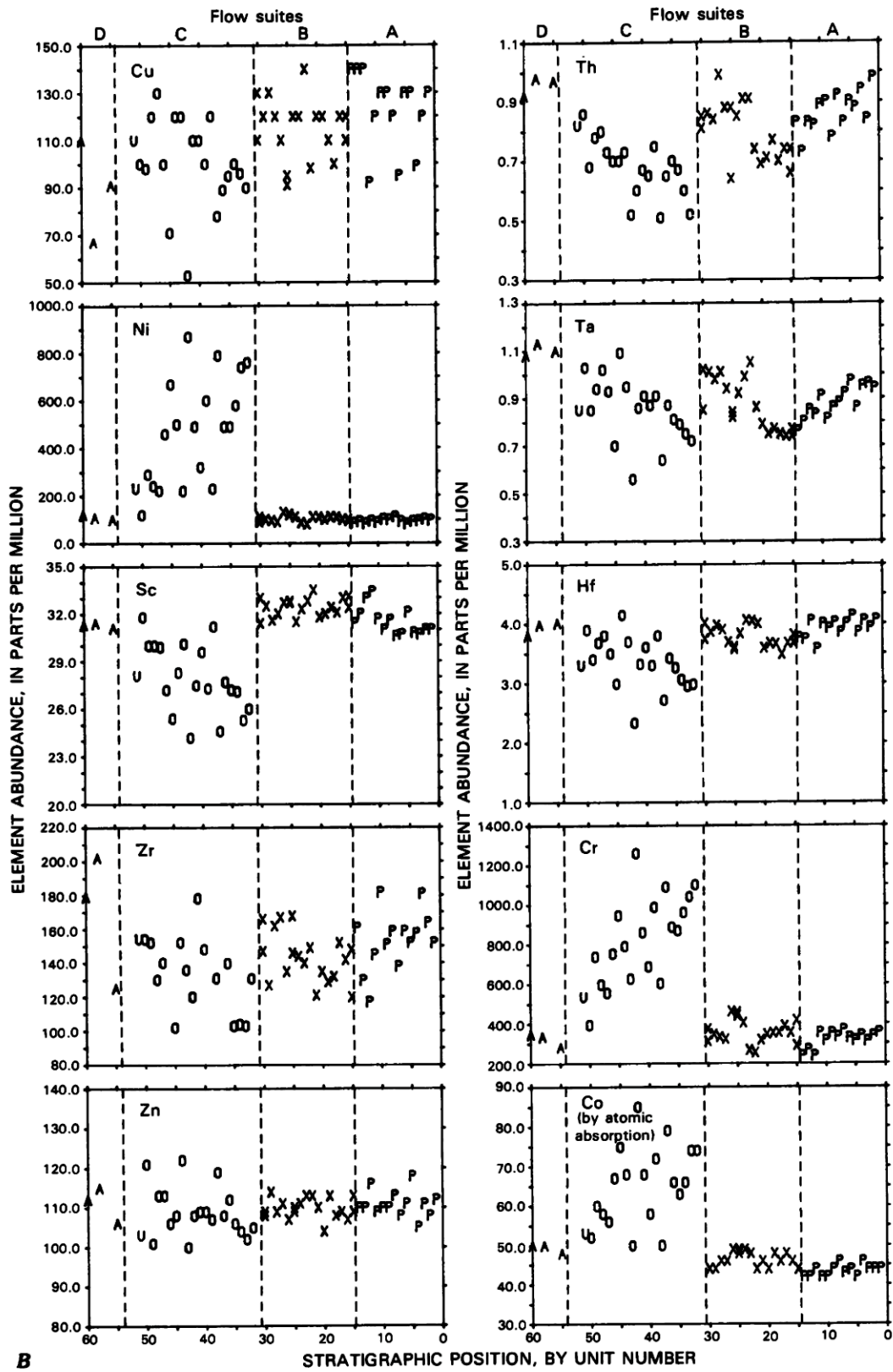


FIGURE 13.6.—Continued.

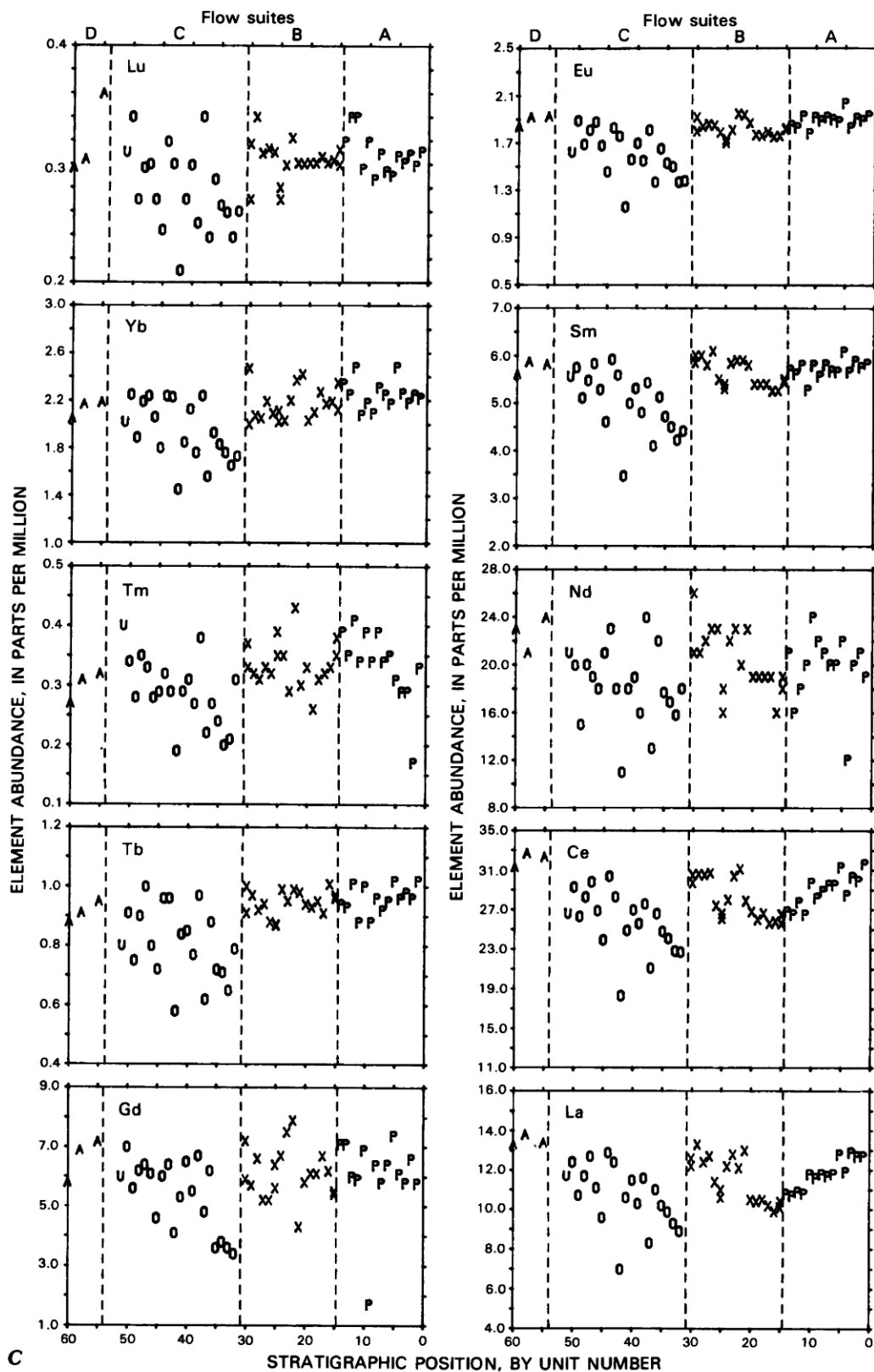


FIGURE 13.6.—Continued.

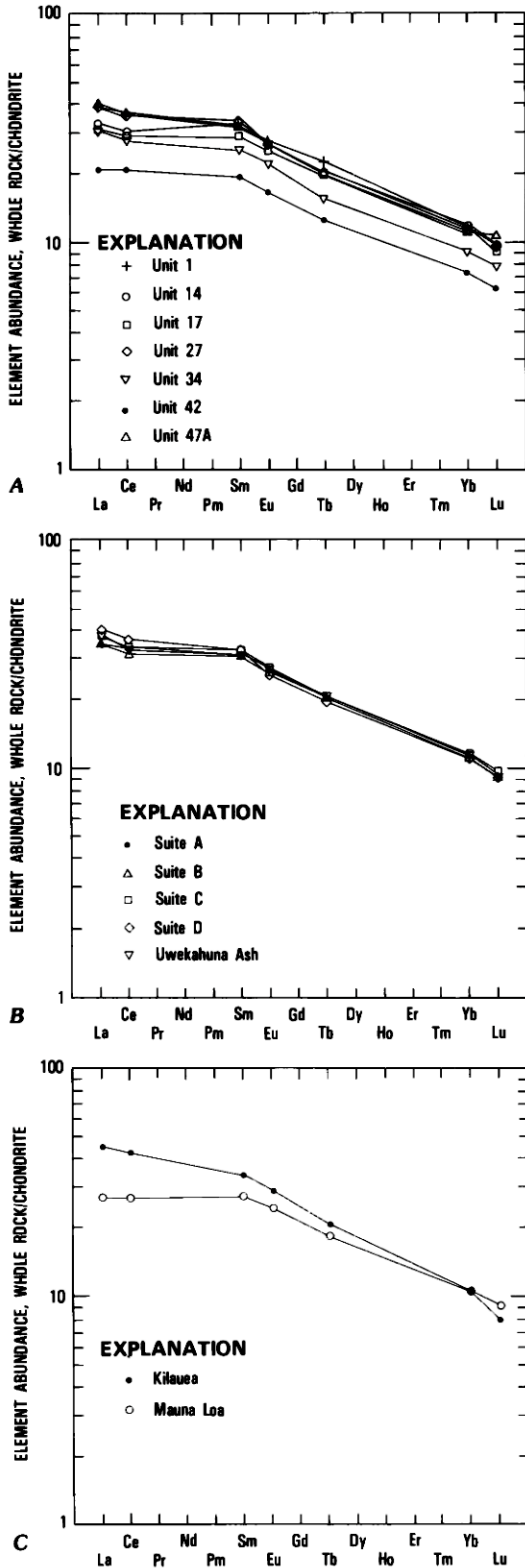


FIGURE 13.7.—Chondrite-normalized abundances of rare-earth elements in Uwekahuna Bluff samples. Abundances are normalized to chondrite values of Haskin and others (1968). Precision for most rare-earth-element (REE) abundances determined by neutron activation (Baedecker, 1979) is better than ± 3 percent of reported value (see text). Precision for Nd, Gd, and Tm is poorer, and

DISCUSSION

SOURCES OF MAGMAS

Flows of suites A and B have broadly similar major-element and trace-element chemistry (fig. 13.6A, B), and we detect no abrupt changes in composition such as might indicate exotic sources. The similarities in the REE patterns for these units likewise suggest a fairly homogeneous source. We interpret these data to indicate that the flows from suites A and B are comagmatic in the broad sense: they were derived from the same magma batch or from different batches with nearly identical source chemistry and crystallization histories.

Because flows of suite C contain various amounts of olivine, MgO content has a range sufficiently wide to define olivine-control lines. Wright (1971) showed that different comagmatic suites may be characterized by different olivine-control lines. The slopes and intercepts for suite C olivine-control lines are comparable to those calculated for various other suites of Kilauea lavas (Murata and Richter, 1966b; Wright, 1971). The similarity of these control lines (fig. 13.8) indicates that olivine is the only significant mineral phase affecting chemical variation in suite C flows and that the composition of that olivine is homogeneous. We interpret the flows of suite C to be derived from a Kilauea source, because their olivine-control lines resemble those of other Kilauea suites.

TRACE-ELEMENT DATA

Abundances of trace elements are similar within a restricted range among the flows from Uwekahuna Bluff and other Kilauea localities. Ba, Rb, Th, Zr, La, Ce, Sm, and Tb values fall within the ranges exhibited by historic Kilauea lavas (fig. 13.9; Basaltic Volcanism Study Project, 1981). No trace-element abundances in Uwekahuna Bluff flows are within the ranges that are unique to Mauna Loa.

The striking similarity among chondrite-normalized curves for each suite (fig. 13.7B) suggests that the magmas for the various suites of flows, as well as for the Uwekahuna Ash member, are comagmatic. They may have a common parent in the upper mantle, have been affected by similar processes after leaving the mantle, or both.

Abundances of light REE are typically lower for Mauna Loa than for Kilauea (fig. 13.7C; Leeman and others, 1977, 1980; Basaltic Volcanism Study Project, 1981), whereas abundances of heavy REE are similar for Kilauea and Mauna Loa lavas. Curves for the flows in Uwekahuna Bluff more closely resemble those for Kilauea than those for Mauna Loa (fig. 13.7B, C). Thus, on the basis of major-, trace-, and rare-earth-element chemistry, it appears that no Mauna Loa flows occur in the Uwekahuna Bluff section.

these elements are not used in plots of chondrite-normalized rare-earth abundances. A, REE abundances in selected flows from Uwekahuna Bluff. B, Averaged and normalized REE data for each suite of flows in Uwekahuna Bluff section and for the Uwekahuna Ash Member. C, Averaged and normalized REE data for historical Mauna Loa and Kilauea flows (data from Basaltic Volcanism Study Project, 1981).

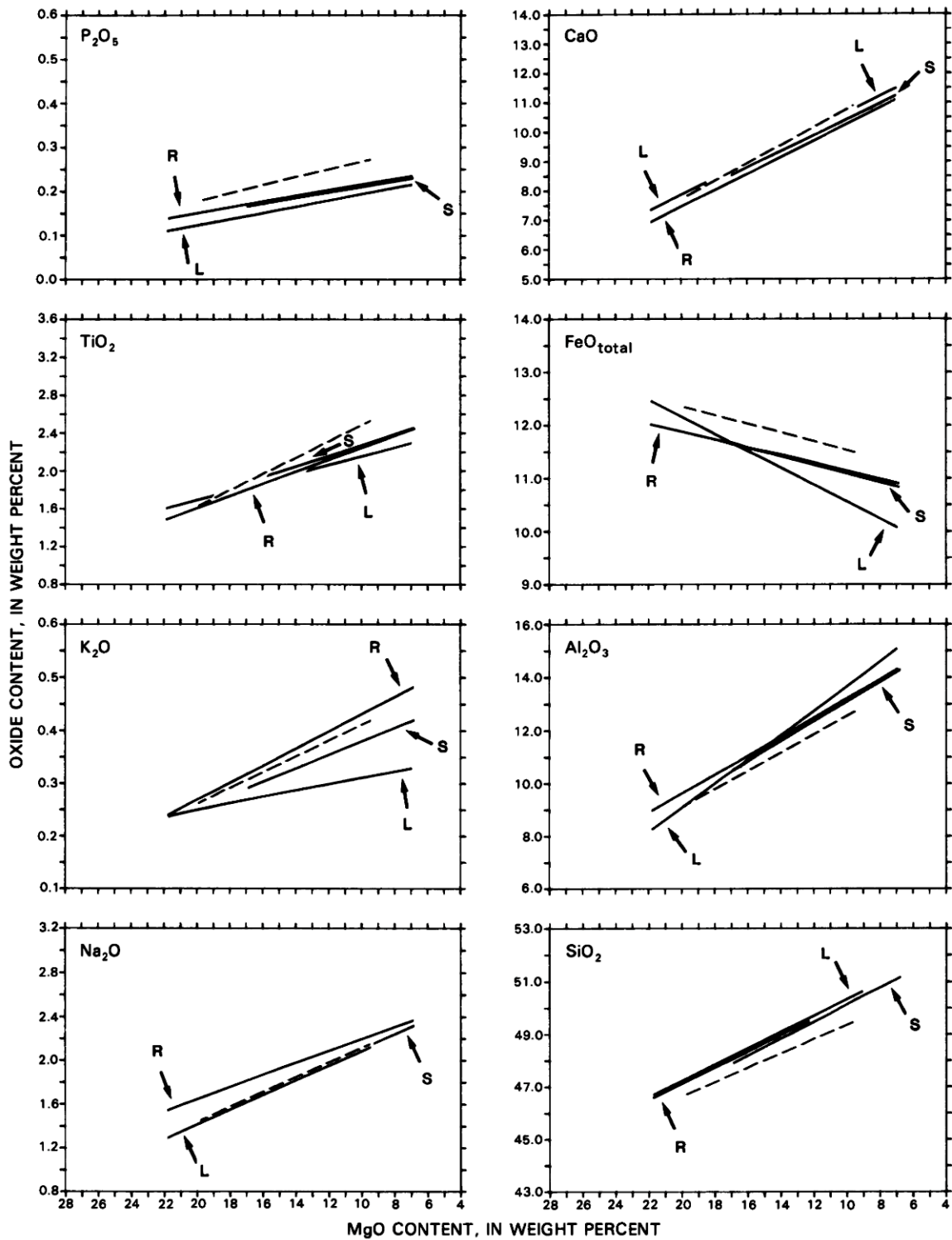


FIGURE 13.8.—Lines of olivine control for Kilauea lavas. Dashed line is for flows of picritic suite C at Uwekahuna Bluff. Other lines labeled by letters: S, Kilauea prehistoric summit lavas (Murata and Richter, 1966a; Wright, 1971); R, Kilauea southwest-rift-zone prehistoric picrites (Wright, 1971); and L, Uwekahuna laccolith (recalculated from data in Murata and Richter, 1961).

SECULAR TRENDS

Olivine control is the dominant mineral control affecting suite C flows. The flows from suites A, B, and D have MgO contents in excess of 6.4 weight percent and show no evidence of fractionation in the sense of Wright and others (1975). We assume that the minor chemical variation displayed by these flows is also olivine controlled. To look for evidence of chemical variability beyond that imposed by olivine control, we recalculated the compositions in table 13.2 to a constant 7.0 weight percent MgO by adding or subtracting olivine from the bulk compositions (Macdonald, 1944; Wright, 1971), using the composition of olivine from the Uwekahuna laccolith (Murata and Richter, 1961). That composition does not account for chrome spinel, which commonly occurs within olivine in Hawaiian lavas, and so we did not recalculate the Cr contents for the Uwekahuna Bluff samples. Listed in table 13.4 are average compositions for each of the lava suites at Uwekahuna Bluff and for juvenile material from the Uwekahuna Ash Member, all normalized to 7.0 weight percent MgO.

The following secular trends are recognized for the Uwekahuna Bluff section (fig. 13.9): (1) SiO₂ increases from 50.2 weight percent for the flows of suite D to 51.1 percent for the flows of suite A; (2) Al₂O₃, FeO, Na₂O, P₂O₅, and MnO remain nearly constant (table 13.4); and (3) CaO and TiO₂ decrease slightly from suite D to suite A. These secular changes differ in sense from those recognized by Wright (1971) for historical Kilauea lavas, in which SiO₂ decreases to the present and CaO and TiO₂ increase.

Historical olivine-controlled flows from Mauna Loa have more SiO₂ and less K₂O, TiO₂, and P₂O₅ than any of the flows from Uwekahuna Bluff (table 13.4; fig. 13.9). The ranges in the contents of these oxides for flows from Uwekahuna Bluff strongly resemble those for historical Kilauea flows.

CYCLIC VARIATIONS IN THE CHEMISTRY OF SUMMIT LAVAS

Plots of chemical composition versus position in the section for lavas of suites A and B (units 1–30) show essentially straight-line relationships (fig. 13.6), but small cyclic(?) departures are discernible. The olivine-rich flows of suite C display considerable scatter in MgO-variation diagrams (fig. 13.5A), but some evidence for cyclicity can be seen when all compositions are normalized to 7.0 weight percent MgO and plotted against stratigraphic position (fig. 13.10). Although the frequency of the apparent cycles varies from element to element, the data do suggest that cyclic variations occur in the compositions of Kilauea summit lavas.

Wright and others (1975) and Wright and Tilling (1980), on the basis of major-element chemistry, identified 10 distinct chemical variants or magma batches among the materials erupted by Kilauea in the period 1968–1974. They interpreted these variants as the unmodified products of separate partial melting events. Hofmann and others (1984) examined trace- and rare-earth-element data from Kilauea for 1968–1971; they concluded that incompatible trace-element concentrations in the lavas fit a pattern of continuous,

TABLE 13.4.—Average chemical compositions of prehistoric lavas and ash from Uwekahuna Bluff, compared with historical Mauna Loa and prehistoric and historical Kilauea

[Recalculated from original analyses by normalizing to 100 percent dry weight after converting all iron to FeO_{total}. Normalized to 7.0 weight percent MgO by subtracting or adding olivine of Uwekahuna laccolith composition (Murata and Richter, 1961, analysis 10). A, suite A flows; B, suite B flows; C, suite C flows; D, suite D flows; UA, Uwekahuna Ash Member, (UA = average of 5 rinds from cored bombs within Uwekahuna Ash Member (Dzurisin and Casadevall, 1986)); Kilauea A (Kil A = Kilauea summit 1911–1924) and Mauna Loa A (MLoA A) (Wright, 1971); Kilauea B (Kil B) and Mauna Loa B (MLoA B) (Basaltic Volcanism Study Project, 1981); n.d., not determined; uncertainty expressed as one standard deviation (1 sigma)]

	A	B	C	D	UA	Kil A	Kil B	MLoA B	MLoA A
SiO ₂	51.10±0.23	50.90±0.39	50.60±0.78	50.23±0.25	51.08±0.35	50.33, n.d.	50.70±0.31	52.45±0.31	52.18, n.d.
Al ₂ O ₃	13.7±0.2	13.6±0.2	13.6±0.3	13.7±0.2	13.73±0.9	14.00, n.d.	13.57±0.12	13.94±0.10	14.17, n.d.
FeO	11.7±0.3	11.8±0.3	11.3±0.5	11.4±0.3	11.63±1.00	11.09, n.d.	11.03±0.20	10.62±0.49	10.94, n.d.
MgO	7.0	7.0	7.0	7.0	7.0	7.0	7.0	7.0	7.0
CaO	10.6±0.2	10.9±0.3	11.7±0.7	11.7±0.4	11.05±0.28	11.58, n.d.	11.65±0.33	10.73±0.15	10.58, n.d.
Na ₂ O	2.4±0.1	2.3±0.1	2.3±0.1	2.3±0.1	2.14±0.25	2.28, n.d.	2.32±0.04	2.36±0.06	2.29, n.d.
K ₂ O	.44±0.02	.43±0.03	.44±0.04	.48±0.03	.45±0.02	.55, n.d.	.53±0.04	.39±0.03	.37, n.d.
TiO ₂	2.51±0.08	2.49±0.12	2.62±0.21	2.68±0.04	2.51±0.09	2.72, n.d.	2.73±0.11	2.10±0.04	2.07, n.d.
P ₂ O ₅	.30±0.01	.29±0.01	.28±0.04	.30±0.01	.26±0.06	.27, n.d.	.29±0.01	.24±0.02	.21, n.d.
MnO	.17±0.02	.17±0.01	.16±0.02	.19±0.01	.16±0.02	.17, n.d.	.17±0.01	.17±0.01	.17, n.d.
Ba	118±19	118±23	127±29	136±11	120±29	n.d.	138±18	84±14	n.d.
Cu	122±16	116±12	119±17	91±22	132±7	n.d.	n.d.	n.d.	n.d.
Hf	3.91±0.14	3.83±0.16	4.02±0.30	3.99±0.08	3.58±0.02	n.d.	4.58±0.17	3.59±0.11	n.d.
Rb	12±3	13±1	16±3	14, n.d.	13, n.d.	n.d.	11±3	6±1	n.d.
Ta	.88±0.06	.88±0.11	1.02±0.10	1.12±0.02	.93±0.05	n.d.	n.d.	n.d.	n.d.
Th	.86±0.07	.81±0.10	.80±0.06	.97±0.02	.89±0.09	n.d.	1.28±0.22	.55±0.03	n.d.
Zn	111±3	111±3	132±14	113±5	112±3	n.d.	n.d.	n.d.	n.d.
Zr	153±17	145±15	156±25	172±41	139±18	n.d.	159±20	130±5	n.d.
Sc	31.4±0.9	32.8±0.7	33.5±1.4	31.8±0.4	30.8±0.2	n.d.	33.0±2.0	31.0±1.2	n.d.
La	11.8±0.8	11.6±1.2	12.7±1.0	13.7±0.3	12.9±0.4	n.d.	15.1±1.7	8.9±0.6	n.d.
Ce	28.9±1.6	28.3±2.0	30.7±1.9	32.7±0.5	28.8±0.5	n.d.	37.5±3.2	23.9±1.4	n.d.
Nd	20±3	21±3	22±3	23±2	23±3	n.d.	n.d.	n.d.	n.d.
Sm	5.7±0.1	5.7±0.3	6.0±0.4	5.9±0.1	6.0±0.1	n.d.	6.2±0.2	5.0±0.2	n.d.
Eu	1.89±0.05	1.84±0.06	1.92±0.10	1.93±0.03	1.74±0.04	n.d.	2.00±0.07	1.69±0.04	n.d.
Gd	6.1±1.4	6.2±0.9	6.4±1.0	6.7±0.7	7.1±0.7	n.d.	n.d.	n.d.	n.d.
Tb	.96±0.04	.96±0.04	.97±0.10	.93±0.03	.90±0.02	n.d.	.96±0.03	.86±0.04	n.d.
Tm	.33±0.06	.34±0.04	.34±0.05	.31±0.02	.34±0.08	n.d.	n.d.	n.d.	n.d.
Yb	2.25±0.11	2.20±0.13	2.31±0.14	2.17±0.06	2.18±0.05	n.d.	2.05±0.03	2.10±0.04	n.d.
Lu	.31±0.02	.31±0.02	.33±0.02	.32±0.03	.31±0.01	n.d.	.26±0.10	.31±0.01	n.d.

VOLCANISM IN HAWAII

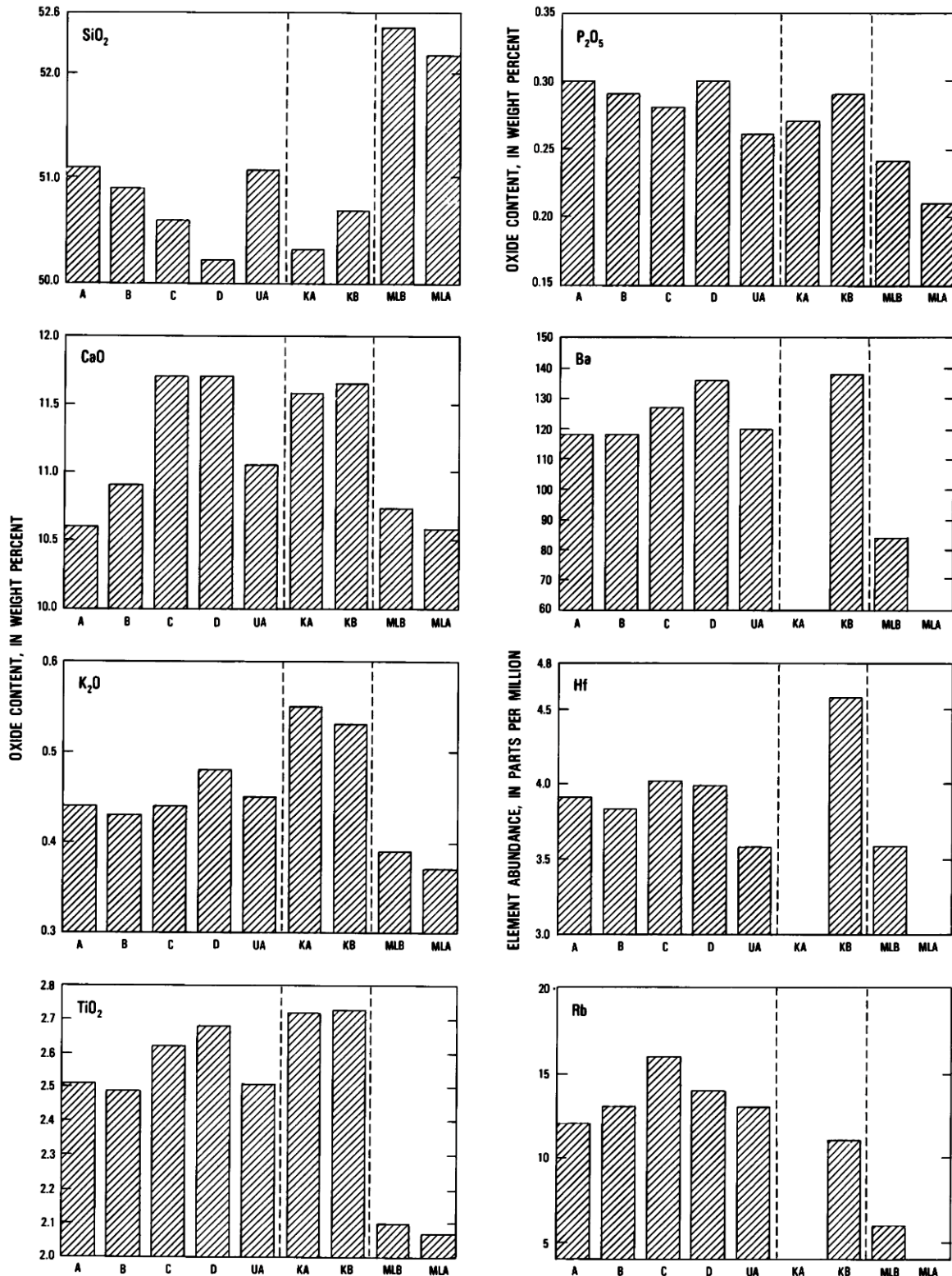


FIGURE 13.9.—Bar graphs showing averaged normalized abundances of selected major oxides and trace elements in Uwekahuna Bluff rocks and in Mauna Loa and Kilauea flows. Averages are recalculated from original analyses by normalizing to 100 percent dry weight after converting all iron to FeO. Averages have been normalized to 7.0 weight percent MgO by subtracting or adding olivine of Uwekahuna laccolith composition (Murata and Richter, 1961, analysis 10). A–D, Suites of flows from Uwekahuna Bluff; UA, Uwekahuna Ash Member; KA, Kilauea

monotonic decrease and that "there was no longer a need to invoke the existence of distinct magma batches to explain either the trace elements or the major elements" (Hofmann and others, 1984, p. 32). Shaw (chapter 51) argues that cyclic behavior on many time scales may be the norm for Hawaiian volcanism and suggests mechanisms to account for such cycles. The apparent cycles at Uwekahuna Bluff are too pronounced to be explained by analytical uncertainty; they

may reflect subtle variations in the chemistry of the parental magma stored in the shallow reservoir.

CHRONOLOGY OF UWEKAHUNA BLUFF

To appreciate more fully the significance of the various rock suites exposed at Uwekahuna Bluff, an understanding of the time

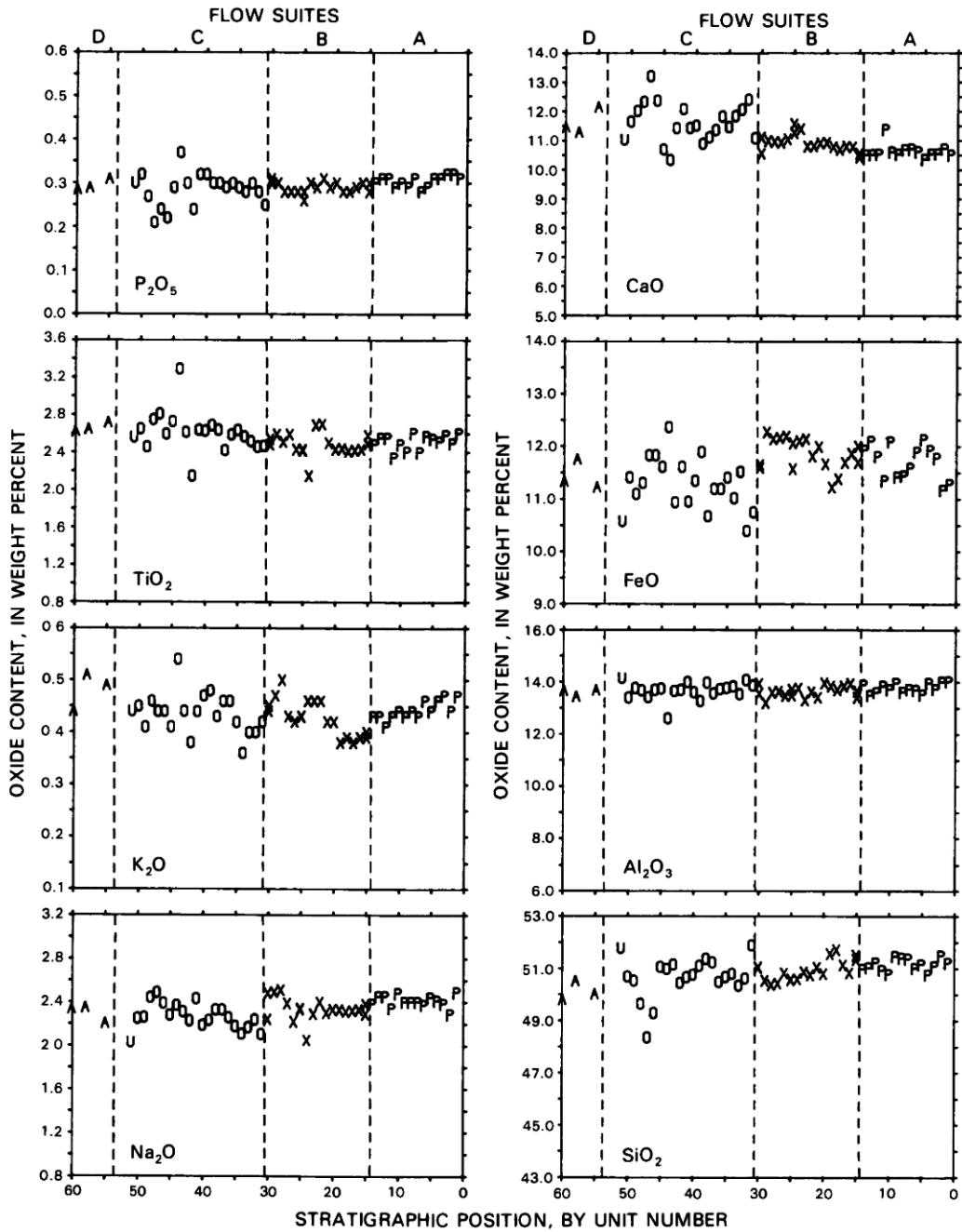


FIGURE 13.10.—Plot of recalculated major-element analyses versus stratigraphic position in the Uwekahuna Bluff section. Analyses have been recalculated to 7.0 weight percent MgO through addition or subtraction of olivine of the composition given in Murata and Richter (1961). Dashed lines separate suites of flows. U indicates sample of the Uwekahuna Ash Member. See figure 13.6 for explanation of other letter symbols.

intervals involved is essential. We offer here a tentative chronology of the sequence at Uwekahuna Bluff and a conceptual model to explain the chemical and petrologic variations observed there.

The Uwekahuna Ash Member, which underlies nearly the entire western wall of Kilauea caldera, is interpreted as the product of large explosive eruptions in the Kilauea summit region about 2.1 ka (Dzurisin and Casadevall, 1986; Lockwood and Rubin, 1986). We found no carbonaceous material within the Uwekahuna Bluff section, so no radiocarbon ages are available for the section above the Uwekahuna Ash Member. However, control on the age of flows within the various suites is available from study of paleomagnetism of the rocks from Uwekahuna Bluff.

Paleomagnetism in the flows of Uwekahuna Bluff has been studied since 1961, when 10 lava flows from the lower half of the section were sampled (Doell and Cox, 1965, 1972). We relocated those holes, which were drilled in units 29, 32, 34, 36, 37, 39, 42, 47A, 48A, and 49A (table 13.1). In 1981, nine additional flows (units 1, 2, 3, 4, 5, 15, 20, 27, and 51) were drilled (R.T. Holcomb and D.E. Champion, unpub. data).

The 1981 samples and the Doell and Cox samples record at least three distinct pole positions (D.E. Champion, oral commun., 1985). Three of the older samples of suite D (units 47A–49A) have paleomagnetic directions consistent with the directions of a lava flow that has been dated at 2.77 ± 0.15 ka (Lockwood and Rubin, 1986; sample W-5345). This age relationship is consistent with the geology of Uwekahuna Bluff, where units 47A–49A underlie the Uwekahuna Ash Member, but it implies a 600–700 yr hiatus in the Uwekahuna Bluff section between the emplacement of suite D flows and deposition of the ash.

A second time unit includes flows 15 through 51 from suites B and C. Flow 51 directly overlies the 2.1-ka Uwekahuna Ash Member. Samples from these flows show a continuous variation in paleomagnetic direction consistent with rapid and steady change of the local magnetic field vector from about 2.1 to 1.5 ka (D.E. Champion, oral commun., 1985). Field evidence indicates no major weathering surface in this sequence of flows. This consistency indicates that the flows of suites C (picrite) and B (aphyric) accumulated in roughly 600 years; no major time breaks are recognized.

The weathered top of unit 15, the uppermost flow of suite B, indicates a hiatus of unknown duration. Paleomagnetic directions within the top five flows of the section (flows of suite A) are consistent with dated field directions of about 0.35 ka (Holcomb, 1981). However, lack of paleomagnetic data for flows 6 through 14 precludes estimating the length of time represented by suite A.

Thus, five major events between 2.8 ka and 0.2 ka are recognized in the Uwekahuna Bluff section on the basis of field occurrence, radiocarbon dating of flows and tephra (Kelley and others, 1979; Lockwood and Rubin, 1986), and paleomagnetic studies (Holcomb, 1981; D.E. Champion, oral commun., 1985). We infer the following eruptive sequence for the rocks exposed at Uwekahuna Bluff:

1. Eruption of aphyric lavas of pre-Uwekahuna Ash Member age (suite D) about 2.8 ka.
2. Eruption of the Uwekahuna Ash Member about 2.1 ka.

3. Eruption of picritic lavas, replenishment of shallow reservoir, and eruption of aphyric lavas (suites C and B) about 2.1 to 1.5 ka (?).

4. Eruption of plagioclase-porphyrific lavas (suite A) about 0.8 to 0.2 ka (?).

5. Formation of present caldera and eruption of Keanakakoi Ash about 0.2 ka.

KILAUEA SUMMIT HISTORY FOR THE PAST 2,800 YEARS

Holcomb (chapter 12) has outlined one sequence of events for the recent evolution of the Kilauea summit area, but alternatives are possible. Our interpretation is generally similar, but we prefer a sequence in which some of the stratigraphic units in Uwekahuna Bluff are older than the ages assigned by Holcomb.

Holcomb (chapter 12) has used paleomagnetic data to assign an age of 2.0–1.5 ka to lava of suite D in Uwekahuna Bluff, as well as several flows outside of the caldera. A similarly magnetized lava flow on Mauna Loa has recently been dated by ^{14}C methods at 2.8 ka (D.E. Champion, oral commun., 1985). As discussed below, we believe that the Uwekahuna Ash Member is older than the 1.5 ka favored by Holcomb and others (in press), so we prefer the age of about 2.8 ka for the lava flows of suite D. These flows should be compared with pre-Uwekahuna Ash Member flows outside of the caldera to see if they may be coeval.

Holcomb (chapter 12) concludes that the present caldera of Kilauea was preceded by an older Powers caldera whose formation may have been associated with explosions that produced the Uwekahuna Ash Member in a manner similar to that proposed for the present caldera and the Keanakakoi Ash Member. The mechanism proposed for this association (Jaggard, 1947; Macdonald, 1965; Christiansen, 1979) involves large-scale summit collapse in response to rapid magma withdrawal into the volcano's rift zones, triggering phreatomagmatic explosions by providing ground water access to the volcano's plumbing system. Though the collapse of the current caldera preceded the explosive Keanakakoi eruption, the interval between collapse and explosion could have been short (Decker and Christiansen, 1983).

Several radiocarbon ages have been determined for the Uwekahuna Ash Member. When the original paleomagnetic chronology of Holcomb and others (in press) was worked out, the available measurements indicated an age of about 1.5 ka. Additional ages have been obtained since then, ranging from 1.0 ka to 2.2 ka. Lockwood and Rubin (1986) argue that the younger ages are affected by sample contamination and adopt 2.1 ka as the most representative age for the ash. Holcomb (chapter 12) prefers to retain the earlier, younger age but we prefer the 2.1-ka ages of Lockwood and Rubin (1986).

Holcomb (chapter 12) suggests that collapse of the Powers caldera was followed by a period of caldera filling which did not affect the Uwekahuna Bluff section for about 0.75 ka, implying that the flows of suite C and suite B are younger than 0.75 ka. D.E. Champion (oral commun., 1985) believes that those flows record continuous variation in paleomagnetic field direction from about 2.1 to 1.5 ka. Dzurisin and Casadevall (1986) argue that the uppermost

pumice of the Uwekahuna Ash Member was buried quickly by picritic lava flows of suite C, because the pumice was uneroded when it was buried. We therefore assign an age of 2.1 to 1.5 ka to suite C and suite B flows and suggest that at least 30 m of suite C flows accumulated rapidly soon after the Uwekahuna Ash Member eruptions.

Our interpretation and that of Holcomb (chapter 12) converge on the age and origin of the suite A flows at Uwekahuna Bluff. These plagioclase-phyric flows are Holcomb's Observatory flows, so named because they form the substrate for the Hawaiian Volcano Observatory. He assigned them an age of 0.25–0.35 ka in figure 12.5, but also noted that they could be as old as 0.75 ka. We suggest that the weathered surface of the uppermost suite B flow records a hiatus of at least a few centuries, and adopt an age of 0.8–0.2 ka for the overlying suite A flows. Following extrusion of the suite A flows, the Uwekahuna Bluff section was capped by the Keanakakoi Ash Member.

The two main differences between our interpretation and that of Holcomb (chapter 12) are: (1) the age of the Uwekahuna Ash Member, and (2) the age and significance of the suite C and suite B lava flows. The differences are caused primarily from differing interpretations of available radiocarbon ages for summit flows and should be resolved by future work.

Our preferred interpretation is that the suite C picrites ponded in the Powers caldera soon after its formation and quickly buried the Uwekahuna Ash Member. Holcomb (chapter 12) agrees that collapse was soon followed by caldera filling, but infers that the Uwekahuna Bluff area was not covered for about 750 years. We interpret the suite C picrites as crystal cumulates or residua from a shallow magma reservoir that was rapidly drained during the Uwekahuna Ash Member eruptions, probably by a large effusive eruption low on the volcano's flank (Dzurisin and Casadevall, 1986). We infer that the lower parts of this magma reservoir were rich in olivine, because of the accumulation of settled olivine crystals (Macdonald, 1944; Murata and Richter, 1966a, b).

Murata and Richter (1966b) proposed that in the 1959 eruption of Kilauea Iki, the eruptive force mobilized olivine sludge from the depths of the shallow reservoir feeding that eruption. Helz (chapter 25) argues that the ascent rate of a juvenile component of the 1959 eruption was sufficient to entrain large olivine grains from a source in the upper mantle. We speculate that the suite C flows at Uwekahuna Bluff represent olivine sludge from the lower part of a compositionally zoned shallow magma reservoir and that unloading during the Uwekahuna Ash Member eruption was responsible for extrusion of the picrites. Preservation at the top of the Uwekahuna Ash Member of a thin pumice layer, which we tentatively assume to be related to emplacement of the ash at about 2.1 ka, indicates that at least 30 m of suite C lava flows accumulated on the floor of the Powers caldera and buried the pumice soon after it was erupted. The absence of weathered flow surfaces at the contacts of suite C flows also implies that most of their 60-m thickness accumulated rapidly after eruption of the ash. This model is attractive because it explains the presence of picrites, which are otherwise unusual in the Kilauea summit area, as a direct consequence of the equally unusual Uwekahuna Ash Member eruptions.

We speculate that the flows of suites B and A ponded within the Powers caldera and that they are genetically related. The plagioclase-porphyrific flows of suite A may represent a later eruptive product of a shallow reservoir that earlier was the source for the aphyric lavas of suite B. We tentatively interpret this sequence of aphyric lavas followed by plagioclase-porphyrific lavas as the product of a two-stage drawdown of a post-Uwekahuna Ash Member shallow magma reservoir. A possible problem with this interpretation is that paleomagnetic evidence suggests a hiatus of at least a few centuries between emplacement of the suite B and the suite A flows, and a hiatus is also indicated by the weathered contact between the suites. According to Holcomb (chapter 12), the hiatus lasted from 0.5 ka to 0.25 ka; according to D.E. Champion (oral commun., 1985) and the model proposed here, the hiatus lasted from 1.5 ka to 0.8 ka.

CONCLUSIONS

We conducted this study in an attempt to answer questions about how the summit region of Kilauea developed: (1) How important were intrusive bodies (sills, laccoliths, and dikes) to the growth of the summit region? (2) Are any lava flows from Mauna Loa exposed in the western wall of Kilauea caldera? (3) Can distinct suites of rocks be recognized in the caldera wall and give a record of the recent chemical evolution of Kilauea summit lavas? (4) Is there any evidence that distinct eruptive centers or source regions have supplied lavas to the summit region during Kilauea's recent past? In terms of these questions, we summarize our results as follows:

(1) Intrusive bodies such as sills and laccoliths are absent at Uwekahuna Bluff. The dikes and laccoliths found elsewhere in the western wall of the caldera account for less than 1 percent of the surface area of the wall (Casadevall and Dzurisin, chapter 14).

(2) The flows of Uwekahuna Bluff are similar in textural variety, phenocryst mineralogy, and major- and trace-element chemistry to prehistoric and historical Kilauea lavas. On the basis of these similarities and the lack of hypersthene, which is found in Mauna Loa flows (Macdonald, 1949), we suggest that all flows within the Uwekahuna Bluff section are from a Kilauea source.

(3) Four distinct suites of flows are recognized at Uwekahuna Bluff on the basis of field occurrence, petrography, and chemistry. Many flows represent near-vent accumulations of fluid lavas. The uniform thickness, lateral continuity, and extensive horizontality of many of the lava flows exposed in the western wall, especially above the Uwekahuna Ash Member, suggest a caldera-fill sequence.

(4) Our data do not require distinct source regions or eruptive centers for the Uwekahuna Bluff lavas, although those possibilities cannot be discounted. We attribute the petrographic differences between lava suites to processes within a single shallow magma reservoir beneath the summit area. The Uwekahuna Bluff lavas could have erupted from a single center or from several in the summit area. Our results are generally compatible with those of Holcomb (chapter 12), but remaining differences of opinion about absolute ages point out the need for additional stratigraphic study.

REFERENCES CITED

- Baedecker, P.A., 1979, Instrumental neutron activation analysis program of the U.S. Geological Survey (Reston, Va.) in Carpenter, B.F., D'Agostino, F., and Yule, H.P., eds., Computers and activation analysis and gamma-ray spectroscopy: Contract 78042, U.S. Dept. Energy, p. 373-385.
- Basaltic Volcanism Study Project, 1981, Basaltic volcanism on the terrestrial planets; New York, Pergamon Press, 1286 p.
- Christiansen, R.L., 1979, Explosive eruption of Kilauea Volcano in 1790 [abs.]: International Association of Volcanology and Chemistry of the Earth's Interior, Symposium on Intraplate Volcanism and Submarine Volcanism, Hilo, Hawaii, July 1979, p. 174.
- Daly, R.A., 1911, Magmatic differentiation in Hawaii: *Journal of Geology*, v. 19, p. 289-316.
- de Saint Ours, P., 1982, Map of tectonic features of Kilauea Volcano summit region, Hawaii: U.S. Geological Survey Miscellaneous Field Studies Map, MF-1368, scale 1:24,000.
- Decker, R.W., and Christiansen, R.L., 1983, Explosive eruptions of Kilauea Volcano, Hawaii, in *Explosive Volcanism: inception, evolution, and hazards*: Washington, National Academy Press, p. 122-132.
- Doell, R.R., and Cox, A.V., 1965, Paleomagnetism of Hawaiian lava flows: *Journal of Geophysical Research*, v. 70, p. 3377-3405.
- 1972, The Pacific geomagnetic secular variation anomaly and the question of lateral uniformity in the lower mantle, in Robertson, E.C., ed., *The nature of the solid Earth*: New York, McGraw-Hill, p. 245-284.
- Dutton, C.E., 1884, Hawaiian volcanoes: U.S. Geological Survey 4th Annual Report, p. 75-219.
- Dzurisin, D., and Casadevall, T.J., 1986, Stratigraphy and chemistry of the Uwekahuna Ash: Product of prehistoric phreatomagmatic eruptions at Kilauea Volcano, Hawaii [abs.]: International Volcanological Congress, Auckland-Hamilton-Rotorua, New Zealand, Abstracts, February 1986, p. 100.
- Dzurisin, D., Koyanagi, R.Y., and English, T.T., 1984, Magma supply and storage at Kilauea Volcano, Hawaii: *Journal of Volcanology and Geothermal Research*, v. 21, p. 177-206.
- Fuller, R.E., 1939, Gravitational accumulation of olivine during the advance of basaltic flows: *Journal of Geology*, v. 47, p. 303-313.
- Gunn, B.M., 1971, Trace element partition during olivine fractionation of Hawaiian basalts: *Chemical Geology*, v. 8, p. 1-13.
- Hanson, G.N., 1980, Rare earth elements in petrogenetic studies of igneous systems: *Annual Reviews of Earth and Planetary Science Letters*, v. 8, p. 371-406.
- Hart, S.R., and Davis, K.E., 1978, Nickel partitioning between olivine and silicate melt: *Earth and Planetary Science Letters*, v. 40, p. 203-219.
- Haskin, L.A., Haskin, M.A., Frey, F.A., and Wildman, T.R., 1968, Relative and absolute terrestrial abundances of the rare earths, in Ahrens, L.H., ed., *Origins and distribution of the elements*: New York, Pergamon Press, p. 889-912.
- Hofmann, A.W., Feigenson, M.D., and Raczek, I., 1984, Case studies on the origin of basalt: III. Petrogenesis of the Mauna Ulu eruption, Kilauea, 1969-1971: *Contributions to Mineralogy and Petrology*, v. 88, p. 24-35.
- Holcomb, R.T., 1981, Kilauea Volcano, Hawaii: chronology and morphology of the surficial lava flows: U.S. Geological Survey Open-File Report 81-354, 321 p.
- Holcomb, R.T., Champion, D.E., and McWilliams, M.O., in press, Dating recent Hawaiian lava flows using paleomagnetic secular variation: *Geological Society of America Bulletin*.
- Jaggard, T.A., 1947, Origin and development of craters: *Geological Society of America Memoir* 21, 508p.
- Kelley, M.L., Spiker, E.C., Lipman, P.W., Lockwood, J.P., Holcomb, R.T., and Rubin, M., 1979, U.S. Geological Survey radiocarbon dates XV: Mauna Loa and Kilauea Volcanoes, Hawaii: *Radiocarbon*, v. 21, p. 306-320.
- Leeman, W.P., Budahn, J.R., Gerlach, D.C., Smith, D.R., and Powell, B.N., 1980, Origin of Hawaiian tholeiites: trace element constraints: *American Journal of Science*, v. 280-A, p. 796-821.
- Leeman, W.P., Murali, A.V., Ma, M.S., and Schmitt, R.A., 1977, Mineral constitution of mantle source regions for Hawaiian basalts—rare earth element evidence for mantle heterogeneity, in *Magma Genesis*: Oregon Department of Mineral Industries Bulletin 96, p. 169-183.
- Lockwood, J.P., and Rubin, M., 1986, Distribution and age of the Uwekahuna Ash, Kilauea Volcano, Hawaii [abs.]: International Volcanological Congress, Auckland-Hamilton-Rotorua, New Zealand, Abstracts, February 1986, p. 112.
- Macdonald, G.A., 1944, The 1840 eruption and crystal differentiation in the Kilauean magma column: *American Journal of Science*, v. 242, p. 177-189.
- 1949, Petrography of the Island of Hawaii; U. S. Geological Survey Professional Paper 214-D, 96 p.
- 1965, Hawaiian calderas: *Pacific Science*, v. 19, p. 320-334.
- Murata, K.J., and Richter, D.H., 1961, Magmatic differentiation in the Uwekahuna laccolith, Kilauea caldera, Hawaii: *Journal of Petrology*, v. 2, p. 424-437.
- 1966a, Chemistry of the lavas of the 1959-60 eruption of Kilauea Volcano, Hawaii: U.S. Geological Survey Professional Paper 537-A, 26 p.
- 1966b, The settling of olivine in Kilauean magma as shown by the 1959 eruption: *American Journal of Science*, v. 264, p. 194-203.
- Peterson, D.W. 1967, Geologic map of the Kilauea Crater quadrangle, Hawaii: U.S. Geological Survey Geologic Quadrangle Map GQ-667, scale 1:24,000.
- Powers, H.A., 1948, A chronology of the explosive eruptions of Kilauea: *Pacific Science*, v. 2, p. 278-292.
- 1955, Composition and origin of basaltic magma of the Hawaiian Islands: *Geochimica et Cosmochimica Acta*, v. 7, p. 77-107.
- Powers, S., 1916, Intrusive bodies at Kilauea: *Zeitschrift fur Vulkanologie*, v. 3, p. 28-33.
- Shapiro, Leonard, 1975, Rapid analysis of silicate, carbonate, and phosphate rocks: U.S. Geological Survey Bulletin 1401, 56 p.
- Stearns, H.T., and Clark, W.O., 1930, Geology and water resources of the Kau district, Hawaii: U.S. Geological Survey Water Supply Paper 616, 194 p.
- Stearns, H.T., and Macdonald, G.A., 1946, Geology and ground-water resources of the Island of Hawaii: Hawaii Division of Hydrography Bulletin 9, 363 p.
- Swanson, D.A., 1973, Pahoehoe flows from the 1969-1973 Mauna Ulu eruption: Kilauea Volcano, Hawaii: *Geological Society of America Bulletin*, v. 84, p. 615-626.
- Swanson, D.A., Christiansen, R.L. 1973, Tragic base surge in 1790 at Kilauea Volcano: *Geology*, v. 1, p. 83-86.
- Walker, G.W., 1969, Geologic map of the Kau Desert Quadrangle, Hawaii: U.S. Geological Survey Geologic Quadrangle Map GQ-827, scale 1:24,000.
- Washington, H.S., 1923, Petrology of the Hawaiian Islands, III: Kilauea and general petrology of Hawaii: *American Journal of Science*, v. 6, p. 338-367.
- Wright, T.L., 1971, Chemistry of Kilauea and Mauna Loa in space and time: U.S. Geological Survey Professional Paper 735, 40 p.
- 1974, Presentation and interpretation of chemical data for igneous rocks: *Contribution to Mineralogy and Petrology*, v. 48, p. 233-248.
- 1984, Origin of Hawaiian tholeiite: a metasomatic model: *Journal of Geophysical Research*, v. 89, p. 3233-3252.
- Wright, T.L., Swanson, D.A., and Duffield, W.A., 1975, Chemical composition of Kilauea east-rift lava, 1968-1971: *Journal of Petrology*, v. 16, p. 110-133.